Ministry of Science and Higher Education
Federal State Autonomous Educational Institution of Higher Education
Kazan Federal University (KFU)

Abdolreza Farhadian

CHALLENGES OF HYDROGEN SULFIDE-INDUCED CORROSION IN THE OIL AND GAS SECTOR

Study Guide

Kazan
2025

UDC 620.193.4

LBC 34.66 i73

A. Farhadian

Challenges of hydrogen sulfide-induced corrosion in the oil and gas sector. A. Farhadian.; Ministry of Science and Higher Education. Kazan Federal University. Kazan: KFU Publishing, 2020. 76 p.

This book considers the issues related to the corrosion inhibition strategies for flow assurance in oil and gas transportation pipelines

This study guide is intended for students in master's program 21.04.01 – Petroleum Engineering, discipline "Flow assurance" and full-time bachelor's program 21.03.01 "Petroleum Engineering".

The book was developed and edited at the Department of Petroleum Engineering in collaboration with the PJSC Tatneft.

Printed by the resolution of the Editorial Advisory Board of Kazan Federal University.

Reviewed by:

Authors

Dr. Abdolreza Farhadian
Head of the Department of Petroleum Engineering, Institute of Geology and Petroleum Technologies, Kazan Federal University

Contents

1. Introduction

Pipeline systems are indispensable components of the oil and gas industry, serving as vital conduits for the conveyance of products to processing plants, storage terminals, and refining complexes [1]. Due to the critical nature of the substances transported within these pipelines, any malfunction or breakdown can result in substantial economic repercussions and environmental harm, along with the potential risk to human safety [2]. Pipeline failures can arise from numerous factors, including various types of corrosion (such as external, internal, and stress cracking), mechanical problems (like material defects, design flaws, and construction mistakes), third-party interference (whether accidental or intentional), and operational challenges (malfunctions, inadequacies, protective system disruptions, or human errors), and natural occurrences (lightning strikes, floods, or land shifts) [3]. Fig. 1 provides an overview of the distribution of failures across a 15-year period (1990-2005) [4]. Corrosion emerges as the leading cause of failures in both natural gas (46.6%) and crude oil pipelines (70.7%). A corrosion cost analysis conducted by a prominent oil and gas company revealed that in 2003, expenses related to corrosion totaled about USD 900 million. Globally, the oil and gas industry's corrosion-related costs amount to roughly USD 60 billion annually, with documented expenditures in the United States alone exceeding USD 1.372 billion.

Given the escalating demand for oil and gas energy resources and associated concerns, the worldwide costs associated with corrosion within this industry are anticipated to further escalate [5]. Consequently, the need for forward-looking risk assessments that balance cost-effectiveness and safety considerations cannot be overstated, as such measures are vital to support the ongoing viability and sustainability of the oil and gas sector while effectively mitigating potential threats to the environment and public welfare.

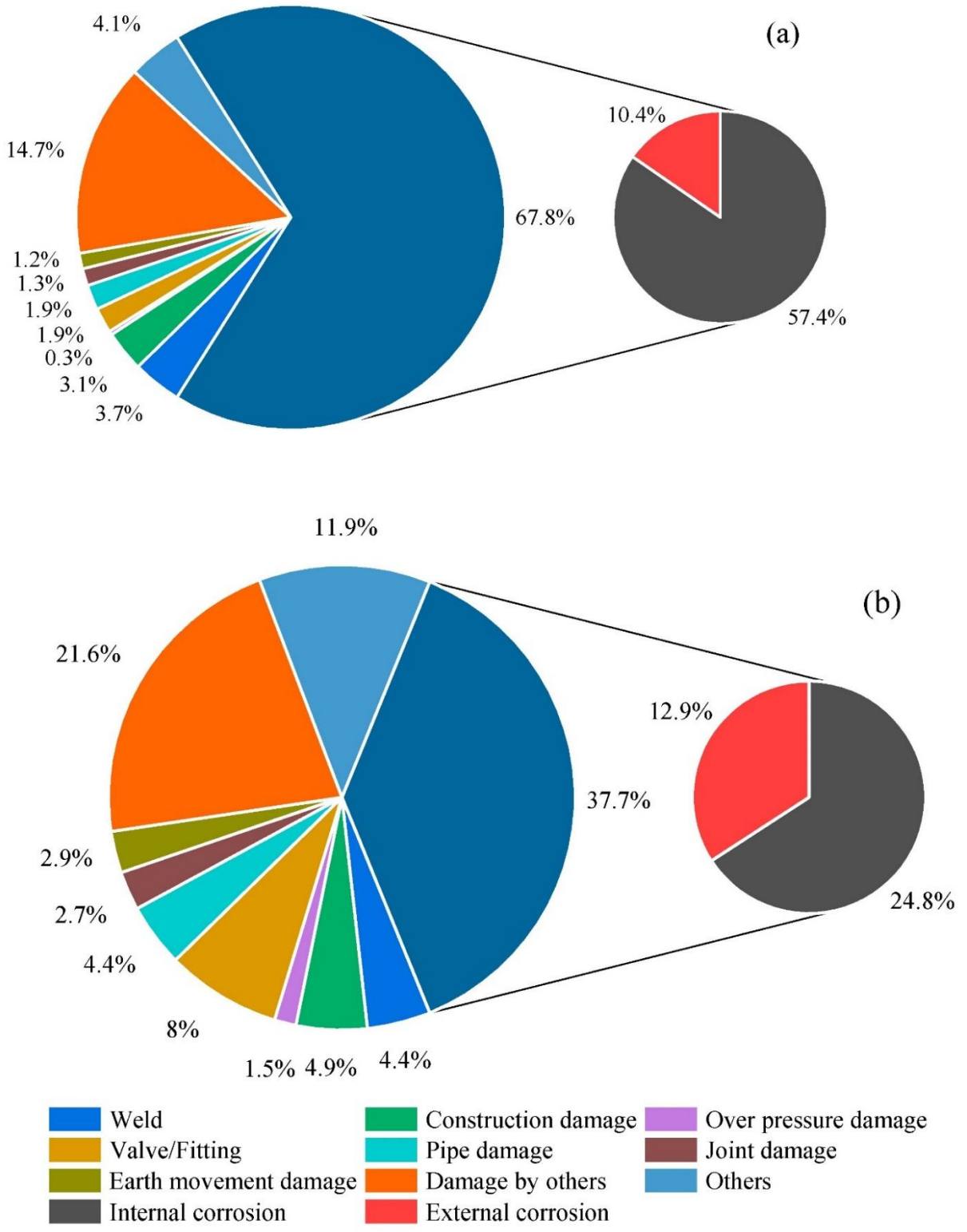

Fig. 1. Pipeline incidents by cause (1990–2005): (a) crude oil (3826 incidents) and (b) natural gas pipelines (411 incidents) [4,5]

The integrity of pipelines is of the utmost importance for ensuring safe operations, protecting the environment, and preserving the operational capabilities of critical production assets. Corrosion poses a significant risk to pipelines, both from external and internal sources. External corrosion can arise due to factors such as oxygen and chloride present in the surrounding environment [6], while internal corrosion may be caused by substances like hydrogen sulfide (H_2S), carbon dioxide (CO_2), and organic acids found in production fluids.

If left unchecked and unmanaged, pipeline corrosion can result in leaks and potentially catastrophic failures [7]. Internal corrosion, in particular, is a major concern within the industry, accounting for approximately 57.4% and 24.8% of corrosion-related failures in crude oil and natural gas pipelines, respectively (Fig. 1) [4]. Therefore, implementing proactive strategies to prevent and control internal corrosion is crucial for ensuring the overall integrity, safety, and long-term sustainability of pipeline operations. Within the oil and gas industry, corrosion is commonly classified into two major categories: sweet and sour corrosion, which occur in environments characterized by high partial pressures of H_2S and CO_2, represented by PH_2S and PCO_2, respectively. These distinct forms of corrosion present considerable challenges for industry professionals. To further understand and classify corrosion types, they are divided into three regimes based on the ratio of PCO_2 to PH_2S:

1. Sweet corrosion: Characterized by a PCO_2/PH_2S ratio greater than 500.
2. Sweet-sour corrosion: A PCO_2/PH_2S ratio ranging between 20 and 500.
3. Sour corrosion: Defined by a PCO_2/PH_2S ratio less than 20:1 [8].

Several critical factors, including H_2S and CO_2 partial pressures (PH_2S and PCO_2), temperature, and pH levels, significantly impact the rate and mechanism of corrosion product formation in sweet and sour environments. These factors influence the dissolution of corrosive gases and, consequently, the overall corrosion process:

- Temperature: Higher temperatures accelerate chemical reactions and increase gas solubility, leading to higher corrosion rates.
- pH: The acidity or alkalinity of the environment, determined by pH levels,

affects corrosion rates. Low pH accelerates corrosion, while high pH can trigger localized corrosion mechanisms.

- Dissolved CO_2 and H_2S: In the presence of water, these gases generate corrosive acids that react with metal surfaces to form less protective compounds, thereby increasing corrosion rates.

In sweet corrosion, metal carbonates ($MeCO_3$) are typically formed [9], whereas various metal sulfides are generated in sour corrosion environments [10]. Corrosion-induced material failures in both sour and sweet conditions present numerous safety, economic, and environmental challenges within the oil and gas industry. As shown in Fig. 2, sour corrosion caused by H_2S is identified as the primary contributor to corrosion-related failures in the 1970s [5]. With the increasing prevalence of sour corrosion over time, it is crucial to proactively address this issue and implement preventive measures to effectively manage associated risks within petroleum industries.

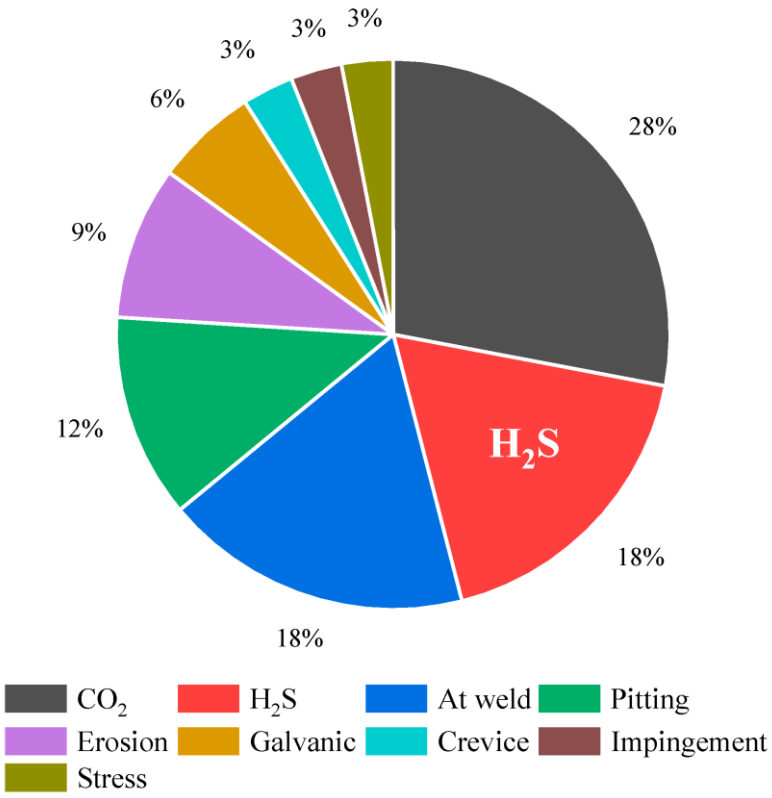

Fig. 2. The primary contributors to corrosion-related failures in the oil and gas industry, along with their respective levels of influence [4,5]

Tackling the issues related to H_2S corrosion in the oil and gas sector is vital because it poses serious risks to equipment, infrastructure, and overall operational effectiveness. H_2S corrosion speeds up the deterioration of equipment, raises the likelihood of structural failures and accidents, and shortens the operational life of assets, leading to expensive repairs or replacements. Moreover, it hampers operational efficiency, leading to decreased production and higher energy consumption.

A comprehensive understanding of H_2S corrosion and the implementation of effective management strategies offer several benefits, including:

- Enhanced safety: By preventing equipment failures and maintaining infrastructure integrity, the likelihood of accidents and environmental incidents is reduced.
- Extended equipment lifespan: Proper management of H_2S corrosion minimizes the need for costly replacements and reduces downtime for repairs.
- Improved operational efficiency: Ensuring efficient and consistent operations minimizes energy consumption and enhances process reliability.

To further advance the management of H_2S corrosion, it is essential to explore emerging technologies and research areas, such as:

- Advanced coating technologies: Developing new protective coatings to mitigate H_2S corrosion.
- Novel materials: Exploring innovative materials with higher resistance to H_2S corrosion.
- Electrochemical processes: Investing in electrochemical techniques to monitor and mitigate corrosion.
- Predictive modeling: Utilizing predictive analytics and continuous monitoring systems to enhance proactive corrosion management.

The application of artificial intelligence and advanced analytics in corrosion management, prediction, and control is a promising area for further exploration. This study aims to consolidate existing knowledge and identify critical research areas related to H_2S corrosion prevention in the oil and gas industries. By identifying key

focus areas and potential technological advancements, it seeks to provide innovative solutions to maintain the integrity and safety of petroleum and natural gas facilities.

This book explores the challenges posed by H_2S corrosion in these industries and evaluates effective mitigation strategies. By examining corrosion mechanisms, identifying susceptible equipment and areas prone to H_2S corrosion, and assessing protective measures, the paper offers valuable insights for researchers and industry professionals in formulating effective corrosion management strategies. The primary objective is to improve the understanding of H_2S corrosion within this industry, identify research gaps, and provide future guidelines to ensure safe and reliable operations.

2. H_2S corrosion in refinery operations

H_2S corrosion in refinery operations frequently originates from sulfur-containing compounds found in natural gas derived from various sources such as crude oil, gas wells, and oil well gas. These compounds encompass thiophenic compounds, sulfur alcohols, elemental sulfur, sulfur ethers, disulfides, and H_2S, as well as more complex sulfides like metal sulfides that feature multiple sulfur atoms or intricate molecular structures. The latter exhibits a broader range of chemical properties and reactivities compared to simpler sulfides, potentially complicating corrosion management efforts. Another critical factor to consider is the role of sulfate-reducing bacteria and other microorganisms, which flourish in specific environments and generate H_2S as a byproduct. These bacteria contribute to the breakdown of sulfur-containing compounds and can also decompose themselves during their formation process, leading to the release of H_2S. Additionally, the thermal decomposition of sulfonate-containing fluids used in oil and gas wells at high temperatures contributes to H_2S production. Collectively, these diverse sources of H_2S pose significant challenges in addressing corrosion risks associated with refinery processes.

H_2S is a toxic, corrosive, and flammable gas with a distinct, pungent odor often described as resembling rotten eggs or cabbage. Despite being colorless, its strong smell makes it easily identifiable. When dissolved in water, H_2S forms hydrosulfuric

acid, which creates a mildly acidic solution. In aqueous media, H_2S readily dissociates into hydrosulfide ions but not sulfide ions [11]. Due to its higher density compared to air, H_2S tends to accumulate in low-lying areas and depressions. Its ignition temperature is commonly recognized as 518 °F (270 °C) [12]. Upon exposure to air, H_2S undergoes rapid oxidation, forming sulfate and sulfur dioxide (SO_2) in the presence of oxidizing agents like radicals. As a result, H_2S has a short atmospheric residence time of approximately 15 days [12]. H_2S has a lower explosive limit of 4% and an upper explosive limit of 44%, indicating that it cannot ignite in air at concentrations below 4% or above 44%. The combustion of H_2S yields SO_2.

Understanding the key physicochemical properties of H_2S is essential for various reasons. Firstly, it ensures safety in industries like natural gas and petroleum where H_2S is present. Knowledge of its corrosive, flammable, and poisonous nature, as well as its characteristic smell of rotten eggs, helps prevent accidents and provide early warnings. Secondly, understanding the physical properties of H_2S enables effective detection methods beyond relying solely on the sense of smell, as olfactory fatigue can hinder detection in low concentrations. This knowledge aids in the development and use of specialized equipment and gas detectors for accurate detection of H_2S. Additionally, knowledge of the physicochemical properties of H_2S is vital for studying its chemical reactions and interactions. This understanding provides insights into its potential biological and clinical effects, such as its interactions with nitric oxide and its impact on cellular processes. Lastly, understanding the properties of H_2S is essential for evaluating its environmental effects and developing strategies to control its release and mitigate associated risks in natural settings. In summary, familiarity with the key physicochemical properties of H2S ensures safety, supports efficient detection, aids in studying its chemical behavior, and assists in managing its environmental consequences.

H2S originates from multiple refinery sources during crude oil processing (Fig. 3). The primary source is crude oil itself, which contains sulfur compounds that release H2S during refining [14]. Crude oil is categorized as "sweet" or "sour" based on sulfur

content, with sour crude containing higher levels of sulfur compounds and H2S.

Other refinery sources that contribute to H_2S production include:

1. Hydrodesulfurization units: These units efficiently remove sulfur from products like jet fuel, diesel, and gasoline, converting sulfur compounds into H_2S [15].
2. Catalytic reforming: This process converts low-octane hydrocarbons into high-octane gasoline blending components and can generate H_2S if sulfur-containing compounds are present in the feedstock [16].
3. Hydrotreating units: Hydrogen gas reacts with hydrocarbon streams in these units, removing impurities such as sulfur and converting sulfur compounds into H_2S [17].
4. Delayed coker units: These units convert heavy residuals into lighter products, including petroleum coke, which can release H_2S [18].
5. Sulfur recovery units (SRUs): Refineries use SRUs to extract elemental sulfur from sour gases produced during refining processes. Incomplete conversion or operational inefficiencies can lead to H_2S emissions [19].
6. Sulfuric acid alkylation units: During the alkylation process, high-octane alkylate is produced using sulfuric acid. Sulfur-containing impurities in the feedstock can result in H_2S formation as a byproduct [20].
7. Tank vents and storage facilities: These facilities, particularly those containing sour crude oil or intermediate products from desulfurization processes, may emit H_2S when vented, especially during filling or maintenance activities [21].
8. Wastewater treatment processes: Refinery wastewater containing sulfur compounds can generate H_2S during treatment due to microbial activity or chemical reactions [22].

Fig. 3 illustrates H2S sources in refineries, including crude oil processing and units like hydrodesulfurization, catalytic cracking, hydrotreating, and delayed coking. Understanding these sources is vital for effective corrosion management and refinery safety.

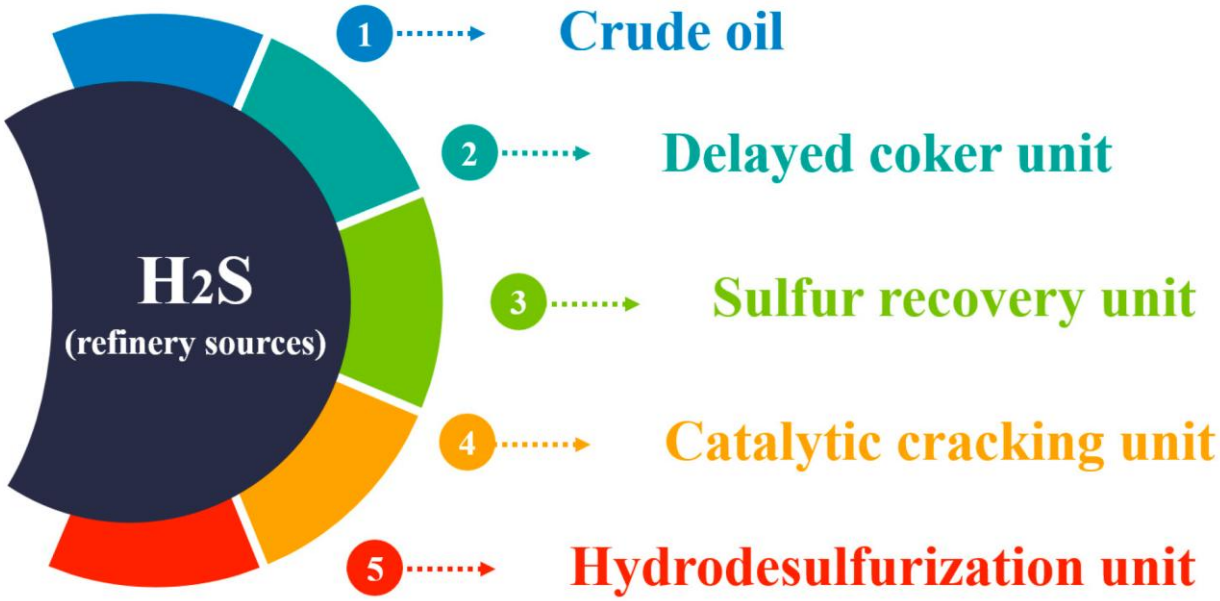

Fig. 3. Main H_2S sources in the refinery [4]

2.1. H_2S corrosion locations

Oil and gas reservoirs with H_2S concentrations exceeding 3 parts per million by volume (ppmv) in the gas phase are classified as sour hydrocarbon systems. In these systems, the presence of H_2S can lead to a type of corrosion known as sour corrosion, which affects downhole tubulars and surface infrastructure in the oil and gas industry [23]. Downhole tubulars, which include pipes and casings used in oil wells, extend from the surface into the wellbore and play a critical role in extracting and transporting oil and gas from underground reservoirs. Surface infrastructure encompasses all above-ground facilities and equipment, including storage tanks, processing units, and other installations involved in oil and gas operations. Sour corrosion presents significant challenges in refineries and other oil and gas facilities, impacting various sections such as downstream equipment, hydrotreating units, catalytic reforming units, sour water strippers, amine units, flare systems, and heat exchangers (Fig. 4). A comprehensive understanding of the vulnerability of these components to H2S corrosion is vital for developing effective corrosion management strategies and maintaining the integrity and safety of oil and gas operations.

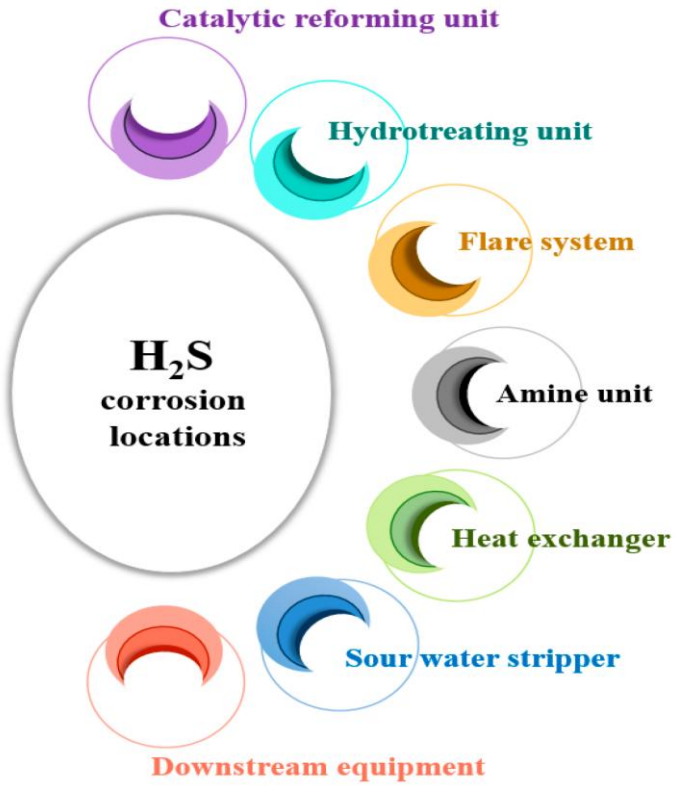

Fig. 4. Specific locations susceptible to H_2S corrosion in a refinery [4]

Liu et al. [24] documented a case where dew point corrosion occurred in the presence of H_2S, causing injection pipes to fracture and perforate. The rupture of these pipes led to changes in the flow rate and temperature characteristics of the overhead pipe. This corrosion was attributed to an unsuitable choice of material for the inhibitor injection tube, given the operational environment. In another instance, a study reported an acid gas and sulfur leakage into the air from a refinery's Sulfur Recovery Unit (SRU) [25]. This incident resulted from heat exchanger malfunctions in the SRU caused by the corrosion of mild steel equipment due to high levels of H_2S in the system. The reaction between H_2S and steel led to the formation of iron sulfide, and upon its removal, pitting was observed on the steel surface. These examples illustrate the damaging consequences of H_2S corrosion on oil and gas infrastructure and emphasize the importance of selecting corrosion-resistant materials and applying robust corrosion management strategies to safeguard the safety and integrity of these systems.

2.2. Mechanism of H_2S corrosion

Corrosion in pipelines that come into contact with sour fluids containing H2S can develop via various mechanisms. The process begins with the dissolution of H_2S gas in water, which creates a highly acidic environment. As H_2S dissolves, it undergoes rapid ionization, producing hydrogen (H^+) and bisulfide (HS^-) ions. Additionally, HS^- ions may undergo further secondary ionization, resulting in the release of additional sulfide (S^{2-}) and hydrogen (H^+) ions [26]. The ionization reaction of H_2S is represented by the following equations:

$$\mathbf{H_2S \rightleftharpoons H^+ + HS^-} \quad (1)$$

$$\mathbf{HS^- \rightleftharpoons H^+ + S^{2-}} \quad (2)$$

The formation of these ions leads to the development of a highly corrosive environment that accelerates the degradation of pipeline materials. Understanding these mechanisms is crucial for developing effective corrosion management strategies to mitigate the damaging effects of H_2S in sour fluid pipelines.

Upon contact with the steel surface, H^+ ions acquire electrons from the metal, leading to a reduction reaction that forms H_2, known as the cathodic reaction. Concurrently, iron in the steel releases an electron and engages in a chemical reaction with S^{2-} ions, resulting in the formation of iron sulfide (FeS), which is considered an anodic process [27]. These collective reactions contribute to steel corrosion, as shown in the following equations:

Cathodic Reaction:

$$\mathbf{2H^+ + 2e^- \rightarrow H_2} \quad (3)$$

Anodic Reaction:

$$\mathbf{Fe \rightarrow Fe^{2+} + 2e^-} \quad (4)$$

$$\mathbf{Fe^{2+} + S^{2-} \rightarrow FeS} \quad (5)$$

Overall Corrosion Reaction:

$$\mathbf{Fe + H_2S \rightarrow FeS + H_2} \quad (6)$$

The aforementioned reactions have notable consequences:

(a) The creation of hydrogen atoms can result in hydrogen embrittlement (HE)

in steel. In the presence of H_2S and/or HS^- ions, the transformation of hydrogen atoms into molecules is impeded. This obstruction leads to an accumulation of surplus hydrogen atoms and elevated pressure.

(b) An increase in the partial pressure of H_2S causes a decline in pH values within the solution. This pH decrease can exacerbate metal corrosion due to the heightened acidity of the surrounding environment.

Both consequences contribute to the degradation of steel in H_2S-containing environments and emphasize the necessity of employing appropriate corrosion management strategies to mitigate these detrimental effects.

2.3. H_2S corrosion products

Hydrogen atoms present in steel can result in HE, particularly when their recombination into hydrogen molecules is hindered by the presence of H_2S and/or HS^- ions. Additionally, increased partial pressures of H_2S can enhance corrosion by raising the concentration of the solution and decreasing its pH value.

In H_2S-containing environments, high-strength steels, such as those used in pipelines and pressure vessels, naturally form an iron sulfide (FeS) film on their surfaces. This FeS film serves as a barrier against hydrogen diffusion and fosters hydrogen reduction reactions due to its advantageous electrical conductivity [26]. The specific type of FeS corrosion product formed depends on factors like temperature, pH, and H_2S concentration. Examples of such corrosion products include troilite, mackinawite, marcasite, pyrrhotite, and kansite [28]. Fig. 5 presents the relative percentages of primary corrosion products resulting from the exposure of carbon steel to H_2S-induced corrosion [5]. This information helps illustrate the complexity of corrosion processes in H_2S-containing environments and highlights the importance of considering these factors when developing effective corrosion management strategies for oil and gas facilities.

A thorough understanding of the different types of FeS corrosion products is crucial for developing effective corrosion prevention and mitigation strategies in H_2S-

rich environments. Different FeS forms exhibit distinct protective properties and behaviors under various conditions. For instance, the formation of a protective film by mackinawite leads to reduced corrosion rates. However, it is essential to consider that changes in process conditions may reintroduce corrosion risks as new mackinawite forms. This knowledge of FeS behavior is vital for engineers and operators working to maintain the reliability and safety of equipment in the petroleum and natural gas industry. Mackinawite is the primary sulfide product in most oil and gas pipelines operating at temperatures below 90 °C. At higher temperatures, troilite and/or pyrrhotite become the dominant corrosion products [29]. Mackinawite forms as the initial corrosion product on Fe in H_2S-rich environments and plays a significant role in corrosion processes. Its formation involves complex chemical reactions between Fe and S^{2-} ions, resulting in a tetragonal crystal structure [30]. The presence of Fe^{2+} ions on its surface makes mackinawite highly susceptible to oxidation when exposed to oxidizing agents. While mackinawite initially reduces corrosion rates, changes in conditions may lead to renewed risks [31]. Considering these factors, understanding the complex chemistry and behavior of FeS corrosion products is crucial for selecting appropriate materials and designing effective corrosion management strategies to ensure the integrity and safety of oil and gas facilities in H_2S-rich environments.

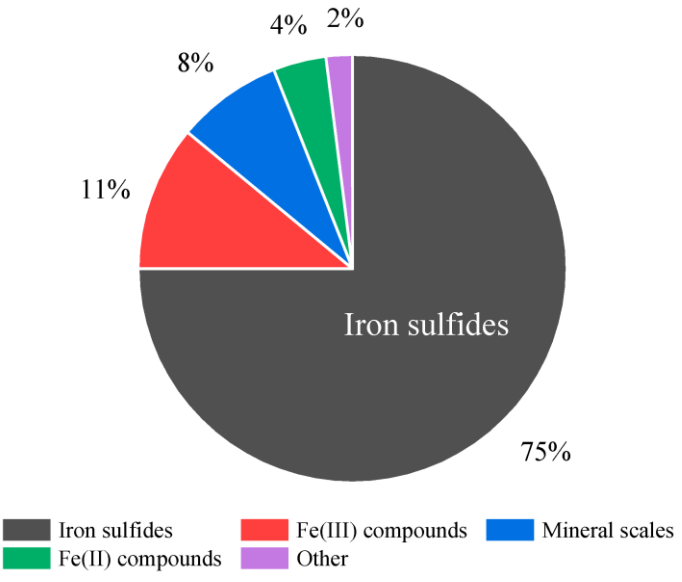

Fig. 5. Common H_2S corrosion products and their relative percentage [4,5]

FeS exhibits unique chemical bonding properties that facilitate the formation of nonstoichiometric polymorphs, characterized by high polarizability and layered structures [32]. Mackinawite rapidly becomes the primary corrosion product on iron immersed in H_2S-containing solutions and gradually transforms into pyrrhotite over time. Studying the behavior of FeS in oxygen-free H_2S solutions, particularly concerning pH and electrode potential, helps us understand their characteristics and stability, contributing to our knowledge of corrosion processes and enabling the development of effective corrosion mitigation strategies [33,34]. Table 1 provides a detailed summary of various FeS types, including their composition, properties, crystal structures, and distribution [5]. Cubic FeS is commonly found in corrosive environments affecting iron-based alloys and certain bacterial species. Its structure closely resembles that of sphalerite, with sulfur atoms forming at the vertices of a face-centered cubic lattice and iron atoms occupying half of the tetrahedral sites. Cubic FeS forms when temperatures drop below 92 °C and pH levels range from 2 to 6, through the interaction between elemental iron and sulfur ions in the aqueous phase [35]. Unlike other FeS compounds, cubic FeS is considered metastable and undergoes phase transitions at room temperature within a few days. Research by Murowchick and Barnes has demonstrated that a pH environment between 4 and 5 and temperatures ranging from 35 to 60 °C promote the nucleation of cubic FeS from competing reactions involving Fe^{2+} and S^{2-} ions. However, the exact mechanism behind cubic FeS formation remains unclear. Within the sphalerite structure, cubic FeS consists of $[Fe_4S_6(H_2O)_4]^{2-}$ groups and the $Fe_4S_6^{2-}$ subunit, which could act as essential precursors in solution. Despite this, cubic FeS has not been observed in nature due to its transient existence [35].

Table 1

Characteristics of different iron sulfides [4,5]

Name	Formula	Lattice Structure
Amorphous FeS	$Fe(HS)_2$, FeS_x	Nan-crystalline
Mackinawite	$Fe_{1+x}S$, x = 0.005–0.025	Tetragonal
Pyrite	FeS_2	Cubic
Greigite	Fe_3S_4	Cubic
Cubic FeS	FeS	Cubic
Marcasite	FeS_2	Orthorhombic
Pyrrhotite	$Fe_{1-x}S$ Fe_7S_8	Hexagonal Monoclinic
Smythite	Fe_9S_{11}, Fe_7S_8	Hexagonal
Troilite	FeS	Hexagonal

Pyrrhotite and troilite are commonly found iron–sulfur minerals with distinct structural properties. Pyrrhotite, the most prevalent Fe-S mineral in the solar system, displays various superstructures based on the NiAs crystal configuration. It typically forms in high-pressure H_2S environments or on metal surfaces with extended service lives, often exhibiting a hexagonal micro-morphology that results in reduced corrosion rates of steel [28,36]. Troilite, a member of the pyrrhotite crystal system, shares similarities with pyrrhotite but possesses a NiAs-type super-structure at room temperature. It undergoes phase transitions, namely α-phase and β-phase transformations, ultimately converting to NiAs unit cells at specific temperatures. Troilite may also exhibit an acicular morphology in H2S environments [37,38]. Greigite, frequently associated with microbial environments, plays a vital role in the directional arrangement of magnetic bacteria [39]. While not commonly found in Fe-H_2S-H_2O systems, it may occur in oxygen-containing environments, although the precise reaction mechanisms behind its formation in such conditions remain unclear. Greigite's anti-spinel structure, similar to ferrous oxide, consists of two sub-lattices of iron atoms and a cubic lattice of sulfur ions, which contribute to its unique properties and behavior [35]. In contrast, pyrite, featuring a cubic crystal structure resembling

NaCl, ranks among the most abundant Fe-S minerals in the Earth's crust. Synthesized strawberry pyrite crystal grains have been observed in Fe-H_2S-H_2O systems, particularly in high-sulfur or high-temperature environments, but not typically in low-H_2S environments. Extensive research on pyrite formation highlights its significance in geological and environmental contexts [35,40].

FeS films are challenging to characterize due to their lack of observable macroscopic crystallinity. Previous studies indicate that amorphous FeS, potentially in the nanocrystalline mackinawite form, serves as a foundational compound for forming other FeS [41]. The protective properties of the FeS film depend on the H_2S concentration and solution pH [42]. A protective FeS film develops within specific pH ranges, inhibiting metal corrosion. Mackinawite forms at room temperature and nearly neutral pH levels, while amorphous FeS precipitates within a pH range of 5 to 7 [43]. Local pH near the metal surface influences FeS precipitation, with non-conductive films such as ferrous carbonate ($FeCO_3$) acting as diffusion barriers against corrosive species. The FeS scale's characteristics are significantly impacted by the quantity of Fe^{2+}, leading to different types of precipitated films with varied protective properties. The film's porosity plays a critical role in regulating corrosion rates under filming conditions, as incomplete films with porosity can create localized metal attack [44].

Researchers have observed that the types of corrosion products formed in H_2S-containing systems depend on the prevalence of mackinawite. When H_2S levels are high, and Fe^{2+} levels are low, mackinawite generally dominates the scale formed on steel surfaces. Conversely, when H_2S levels are low and Fe^{2+} levels are high, both $FeCO_3$ and mackinawite can emerge [44]. The presence of H_2S exacerbates pitting corrosion, leading to the formation of FeS islands such as mackinawite and possibly smythite within the porous $FeCO_3$ layer [41]. Understanding the transitions between corrosion products, like the shift from mackinawite to smythite, is crucial for corrosion control, considering the potential resurgence of corrosion and its subsequent impact on equipment integrity.

As H_2S levels increase, the composition of the corrosion product layer shifts

from $FeCO_3$ to mackinawite. Mackinawite films rapidly grow under sufficient H_2S concentration, forming a thin, continuous layer directly on the steel surface due to the chemical interaction between H_2S and steel [41]. The initial formation of a mackinawite film on the steel surface provides protection and significantly reduces the corrosion rate caused by carbonic acid (H_2CO_3) [45]. Over time, the FeS film becomes denser and more crystalline as H_2S penetrates the mackinawite layer from the surrounding solution towards the steel surface, causing exfoliation. During this process, an outer layer with fractures and porosity forms [45]. Ferrous ions from areas without a mackinawite film migrate and precipitate within the porous film and on its outer surface, leading to mackinawite formation.

Interestingly, the overall iron concentration within the sulfide film often appears lower than the iron depleted due to corrosion, suggesting migration of FeS or other Fe compounds away from the corroded area. Localized corrosion occurs when the protective sulfide film deteriorates, usually due to mechanical instability or damage, especially in high chloride environments. Over time, the mackinawite film may undergo transformations, changing from mackinawite and smythite to different sulfides, leading to fracture of the sulfide film and subsequent exposure of the steel surface, typically at grain boundaries. This initiate localized corrosion [46].

When a non-adherent Mackinawite layer is electrically bonded to a steel surface, hydrogen is generated on the Mackinawite during the cathodic process. The main source of acidity in the water phase comes from the dissociation of H_2CO_3. Different forms of FeS lead to varying levels of corrosion when in close contact with a steel surface. Once a certain corrosion threshold is exceeded, the FeS becomes inactive. However, changes in process conditions can trigger the reactivation of dormant sulfides, causing renewed corrosion. This reactivation phenomenon is especially important for mackinawite and smythite due to their increased vulnerability to corrosion upon reactivation. Exposing dormant sulfides to vacuum and mild heat can initiate the reactivation process, potentially raising corrosion rates [46]. The effectiveness of the mackinawite layer in providing protection depends on the balance

between mackinawite formation and the corrosion rate. Under stable operating conditions, the tendency for corrosion is anticipated to decrease over time as mackinawite and smythite transform into pyrrhotite and troilite. This shift is attributed to the less reversible nature of hydrogen bonding on these sulfides. However, changes in process conditions may stimulate the formation of new mackinawite, resulting in renewed corrosion. This resurgence of corrosion on previously dormant sulfides is often caused by changes in process conditions [46]. Grasping the intricate interactions between FeS polymorphs and their reactivation under different conditions is crucial for developing effective corrosion management strategies and maintaining the long-term durability of materials in environments containing hydrogen sulfide.

3. H_2S corrosion type

Environmental factors significantly influence hydrogen-induced embrittlement caused by H_2S, leading to material fragility. The primary forms of cracking associated with this phenomenon include sulfide stress cracking (SSC) and hydrogen-induced cracking (HIC). These cracking modes can arise from various factors such as the presence of sour gases in pipelines, operational conditions, and material properties. Steel pipelines, widely employed in the transportation of oil and gas, are especially vulnerable to severe environmental conditions, such as microbial-induced corrosion, aggressive anions such as chloride, organic compounds, and acid gases like H_2S and CO_2. These factors make pipelines prone to corrosion, which produces hydrogen as a byproduct. During corrosion, steel oxidizes at the anode, generating Fe^{2+} ions that interact with H_2S to create FeS precipitates. At the same time, hydrogen ions from the dissociation of H_2S generate hydrogen gas at the cathodic site. However, H2S impedes the formation of hydrogen molecules from H^+ ions, reducing hydrogen production at the steel surface [47]. Some of the atomic hydrogen combines to create hydrogen gas, while the rest penetrates the steel's microstructure. The presence of a recombination inhibitor like H_2S, however, obstructs the recombination of atomic hydrogen, resulting

in substantial hydrogen diffusion into the metal [48].

Dissolved hydrogen can have several adverse effects on steel:

1. Hydrogen atoms tend to recombine at voids and inclusion interfaces within the steel matrix, forming molecular hydrogen that becomes trapped and cannot desorb. This can lead to an accumulation of hydrogen partial pressure, potentially causing blister formation. Blisters are a common failure mode, particularly in low-carbon steel containing elongated inclusions near the steel surface.
2. When hydrogen gets confined within parallel lamination planes, it can initiate small cracks associated with HIC. These microcracks may accumulate and align along residual stresses, promoting crack propagation. This phenomenon is known as stress-oriented hydrogen-induced cracking (SOHIC).
3. Even small amounts of hydrogen, typically measured in parts per million (ppm), can cause embrittlement in high-strength steels under external or residual stress, resulting in SSC.

3.1. Hydrogen-Induced Cracking (HIC)

HIC, also known as hydrogen blistering, is a major threat to pipeline steels used for transporting hydrocarbons contaminated with acids [49]. HIC involves the recombination of diffused atomic hydrogen within steel, particularly at structural irregularities like elongated inclusions aligned parallel to the pipeline's surface. Over time, hydrogen molecules accumulate at inclusion interfaces, causing internal hydrogen partial pressure and blister formation [50]. This complex process entails hydrogen diffusion into the steel, gas pocket formation, and subsequent pressure buildup, ultimately leading to pipeline cracks and failure. Several factors significantly impact HIC, including steel composition, pressure, temperature, and hydrogen concentration [51]. Thus, implementing proper pipeline design, maintenance, and monitoring strategies is crucial for reducing hydrogen-induced cracking risks. HIC is a slow process occurring over several years and is unaffected by external stresses. Failure happens when blisters or small cracks form in successive layers and

interconnect. Low-strength steel with high levels of elongated sulfide inclusions is highly susceptible to HIC. However, adding microalloying elements can help decrease this vulnerability in steel. Reducing sulfide content to less than 0.003 wt% substantially lowers the risk of HIC [52]. The concentration of H2S in the environment plays a vital role in controlling HIC, acting as a corrosion catalyst and hindering the recombination process, accelerating atomic hydrogen diffusion within the steel. Steels with high densities of reversible hydrogen traps are more prone to HIC due to higher concentrations of mobile hydrogen. HIC formation is a common type of damage expected in H_2S-containing environments [53]. This cracking occurs internally without external loads, facilitated by elemental hydrogen absorption and subsequent internal recombination processes. Several microstructural factors influence the material's ability to absorb hydrogen, hydrogen diffusion within the material, and susceptibility to HIC. Understanding the threshold concentration of H_2S that promotes cracking is essential for evaluating structures operating under sour environment-like conditions. Cracking typically happens near internal metal discontinuities when the diffusing hydrogen concentration exceeds the threshold [54]. Carbon steel wires, composed of intermediate- to high-carbon steels containing 0.3 to 0.7 wt% carbon, experience non-uniform plastic strain distribution during shaping, leading to significant residual stresses across the wire thickness, affecting mechanical properties [55,56]. Steel susceptibility to HIC is closely linked to microstructural characteristics and hydrogen atom interactions with the metallic matrix [54]. Research suggests that steel composition and nonmetallic inclusion presence contribute to HIC susceptibility [57]. Steels with banded pearlitic structures are more susceptible to cracking than those with a random structure [59,60]. Considering this knowledge aids in understanding broader HIC implications across various steel applications and emphasizes the importance of implementing tailored preventive measures and selecting appropriate materials.

In summary, hydrogen blistering is a complex and potentially detrimental phenomenon in pipelines, involving the diffusion of hydrogen atoms into the metal and the formation of gas-filled cavities. Understanding the mechanisms behind the

initiation and progression of hydrogen blistering is crucial for developing effective prevention and mitigation strategies, considering its potential to cause structural damage and catastrophic failures in pipeline systems. A comprehensive understanding of this phenomenon will enable the development of tailored approaches to ensure the long-term integrity and reliability of pipeline infrastructure.

3.2. Sulfide Stress Cracking (SSC)

SSC has been recognized as a significant problem and a primary cause of failures in pipeline steel in high H_2S environments [61,62]. This issue requires close attention due to the potential for ruptures in high-pressure gas transmission pipelines. SSC typically occurs unexpectedly during operations, highlighting the need for risk-based safety measures in facilities dealing with corrosive fluids. Consequently, ongoing efforts aim to improve management strategies to address this concern effectively [63]. SSC results from the combined influence of three main factors: the presence of susceptible materials, localized tensile stress exceeding a critical threshold, and exposure to a wet, sour, and corrosive environment. In H_2S-rich environments, hydrogen atoms infiltrate the material lattice, facilitated by H_2S catalysis. This occurs through breaches in the protective layer and the formation of small molecular openings on the metal surface. The primary anodic process in the acidic corrosion of steel in the presence of H_2S is the electrochemical dissolution of iron, which releases surface electrons. These electrons are absorbed by hydrogen atoms, enabling them to combine and form molecular hydrogen. The permeation of molecular hydrogen through the protective film causes pitting corrosion on the steel surface, leading to potential discrepancies and the formation of galvanic cells, initiating the corrosion process. As the surrounding area deepens, cracks form under stress, temporarily halting fracture propagation upon encountering ductile material. However, hydrogen diffusion at the crack tip perpetuates the cycle, resulting in crack propagation through mechanical tearing. Steel susceptibility to SSC arises from the diffusion of atomic hydrogen, which originates from the cathodic partial reaction during corrosion in an H_2S-containing

environment [64]. The presence of H_2S hinders the formation of hydrogen molecules and facilitates their diffusion into the steel lattice, reducing the steel's ability to withstand deformation under residual or external stress [64]. Several factors, including steel metallurgy, stress levels, pH, H_2S partial pressure, and chloride ion presence, are crucial in determining steel susceptibility to SSC [65]. In contrast to HIC, which may take years to cause failure, SSC can initiate and lead to failure within hours. The examination of secondary phases along grain boundaries, known as grain boundary precipitates, has been extensively explored in materials science and engineering [64]. These precipitates substantially alter material properties, including mechanical, electrical, and corrosion resistance attributes. Understanding the mechanisms governing their formation and growth is essential for designing and optimizing materials with desired characteristics. Investigating grain boundary precipitates presents opportunities for enhancing material properties, particularly in high-temperature applications, and remains an active area of research and development [64].

SSC involves several stages: hydrogen reduction, adsorption, diffusion, bonding with grain boundary inclusions, and propagation under stress gradients. Heat-affected zones (HAZs) around welds are often susceptible to SSC due to inadequate control of hard phase growth during welding processes [66]. In welding procedures like single-pass fillet welds, HAZs are especially prone to SSC, particularly in low-strength steel, primarily because of insufficient heat input and improper preheating of the base metal. This vulnerability underscores the importance of using multiphase welding techniques with higher heat input and appropriate base metal preheating. Such methods effectively manage hard zone formation in the HAZ, thereby enhancing weld resistance to SSC [67]. Moreover, metallurgical transformations involved in shaping weld joints can considerably impact the microstructure and properties of the metal, particularly within the HAZ. Rapid cooling rates in the weld joint lead to increased lattice defects in both the HAZ and weld zone, intensifying electrochemical activity in these regions. As a result, the HAZ becomes a sensitive area for SSC, increasing its likelihood. The susceptibility of base metal and weld joints to SSC under different

potentials emphasizes the critical role of proper welding techniques in mitigating SSC risks [68]. The understanding of SSC mechanisms and its contributing factors is essential for implementing adequate preventive measures in pipeline construction and maintenance. This knowledge helps guide the development of appropriate material selection, welding procedures, and operational practices to ensure structural integrity, reduce failure risks, and enhance overall pipeline safety in H_2S-rich environments.

3.3. Stress-Oriented Hydrogen-Induced Cracking (SOHIC)

SOHIC mainly occurs in low-strength steels with high residual stresses, particularly at welds in pipelines, presenting a rare but significant challenge in industries operating in H_2S environments [69]. SOHIC shares similarities with HIC and SSC, characterized by a stacked array of cracks traversing the material thickness, significantly reducing the load-bearing capacity of components and leading to substantially higher crack growth rates than HIC [70]. Research by Haidemenopoulos et al. [69] on riser steel operating in wet H_2S service conditions revealed that SOHIC cracks initiate from welded zones and propagate along the rolling direction in the middle of the pipe thickness, influenced by severe wet H_2S conditions and complex stress triaxiality. SOHIC represents a unique manifestation of SSC, emerging from pre-existing microcracks induced by hydrogen under tensile stress perpendicular to the direction of the crack. It typically affects carbon steels in wet, sour environments subjected to applied stress [67]. SOHIC often initiates near the weld zone due to residual stresses, even without inclusions and metallurgical defects, and results from hydrogen accumulation, forming minor cracks that propagate under applied stress [71]. Table 2 provides a comparative analysis between HIC and SSC [66], highlighting the distinct characteristics, mechanisms, and influencing factors of each type of cracking. Recognizing the distinctions between these cracking phenomena is essential for developing and applying effective prevention and mitigation strategies in pipeline design, construction, and maintenance. This understanding ultimately enhances the long-term reliability and safety of pipeline infrastructure in H_2S-rich environments.

Table 2

Comparative analysis of SSC and HIC characteristics [4]

	SSC	HIC
Material strength	Mainly in high-strength steel	Mainly in low-strength steel
Applied stress	Affects severely	No effect
Crack direction	Perpendicular to stress	Dependent on microstructure
Location	Anywhere	Ingot core
Environment	Can occur even in mildly corrosive media	Highly corrosive conditions, appreciable hydrogen uptake
Microstructure	Critical effect, Q and T treatment enhances SSC resistance	Cleanliness and nonmetallic inclusions are critical

In practical scenarios, HAZs near the weld are susceptible to SSC and SOHIC. To mitigate these issues, strategies such as preheating the base metal, using low-hydrogen electrodes, applying a low welding current, and considering post-weld heat treatment can be employed. Even though SOHIC is less well understood than HIC and SSC, it remains a significant concern in sour service environments. A thorough understanding of the factors, beyond inherent resistance, that influence its occurrence is necessary. Spirally welded pipes are particularly prone to SOHIC due to their high residual stresses from welding and forming processes. Moreover, SOHIC is strongly associated with highly aggressive sour conditions, worsened by the presence of elemental sulfur. This hinders the hydrogen recombination reaction, leading to increased hydrogen charging into the steel. However, practical guidelines for preventing SOHIC across material, manufacturing, and fabrication domains are currently lacking, emphasizing the ongoing need for research and development efforts to improve understanding and mitigate the risks associated with SOHIC in H_2S environments [70,72]. For a comprehensive understanding, Fig. 6 provides an

overview of the various forms of internal corrosion resulting from H_2S exposure in pipelines. Comprehending these different corrosion types and their underlying mechanisms is crucial for designing effective prevention and mitigation strategies to ensure pipeline integrity and long-term reliability in H_2S-rich environments.

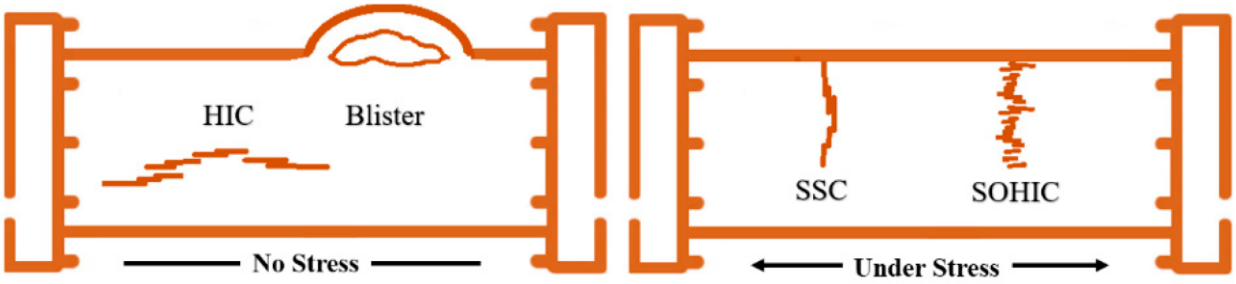

Fig. 6. Significant cracking damage caused by H_2S corrosion [4].

4. Factors affecting H_2S corrosion

Several factors significantly influence both the occurrence and rate of H_2S corrosion. The formation of a thin, protective layer primarily composed of FeS, often in the mackinawite form, is essential for preventing corrosion. The development of this passive film is directly related to the corrosion rate. Although other FeS scales such as pyrrhotite, pyrite, and cubic FeS may also be present, they generally exhibit lower adhesion and greater porosity compared to mackinawite. The ability to form and maintain an adhesive scale is affected by various factors, including temperature, H_2S levels, water impurities, material and electrolyte properties, fluid flow rates, solution pH, and steel chemical composition [29].

4.1 Effect of temperature

Higher temperatures reduce the corrosion resistance of stainless steel because they lead to the formation of passive films with more defects. This is beneficial in moderating the presence of aggressive ions within the passive film, which speeds up the dissolution process and improves the exchange kinetics between the electrolyte and the electrode surface. The temperature also creates a porous film, resulting in reduced

corrosion resistance [73]. Temperature significantly impacts H_2S corrosion in the environment, increasing corrosion rates and reactivity. Higher temperatures cause faster corrosion rates due to enhanced diffusion of corrosive species and elevated H^+ concentration within the acidic environment (10–25 °C). This increased reactivity intensifies corrosion on metal surfaces, establishing a direct relationship between temperature and the corrosion process. Additionally, higher temperatures exacerbate H_2S corrosion by accelerating chemical reactions, particularly beyond 90–100 °C. Fig. 7 summarizes the effects of elevated temperatures on H_2S corrosion, including increased reactivity and intensified corrosion rates.

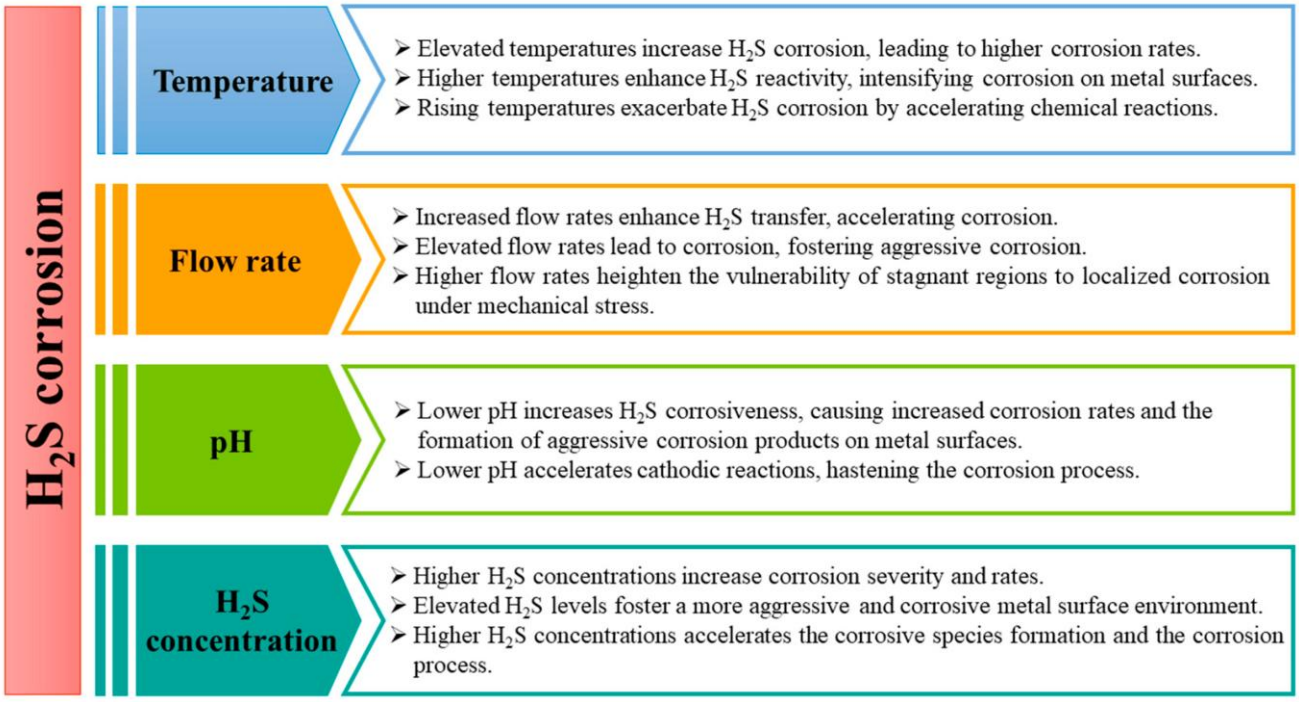

Fig. 7. Impact of Key Factors on H_2S Corrosion [4].

Medvedeva et al. [74] found that H_2S in the environment raises the corrosion rate by 1.5 to 2 times within a temperature range of 20 to 80 °C. Zhang et al. [75] observed that the presence of H_2S makes 316 L stainless steel less protective and more sensitive to temperature, while Silva et al. [76] noted severe corrosion of 316 L stainless steel welded plates at temperatures above 200 °C. Research on carbon steel by Gao et al. [77] revealed an increase in initial corrosion rates from 2 mm/y to 4 mm/y, eventually stabilizing. The relationship between temperature and corrosion exhibits a

complex pattern. At higher temperatures (>100 °C), a decline in corrosion is observed, attributed to higher transport resistance of the corrosion film and reduced H^+ concentration. Mechanisms at elevated temperatures involve reduced gas solubility, leading to increased pH, changes in film formation kinetics, and alterations in corrosion processes at the metal-brine interface. Over time, the development of an FeS layer reduces the impact of temperature on the corrosion process, with mackinawite and Fe_3O_4 consistently forming after brief exposure periods. Research suggests that oxide films formed at 250 °C should be more corrosion-resistant and thicker than those formed at room temperature. However, it is important to note that while the formation of an FeS layer indicates the dominance of "direct" or "solid-state" reactions influencing the corrosion process, the interplay of elevated temperatures and variations in pH levels can induce thermodynamic modifications. These alterations may lead to the deterioration of the protective H_2S film, initiating and progressing the formation of pits across the metal surface.

4.2. Effect of flow rate

The rate of corrosion on metal surfaces induced by H_2S is significantly influenced by the flow rate, particularly in industries such as oil and gas production. Studies conducted by Sun et al. [78] reveal that increasing the fluid velocity leads to higher initial corrosion rates, although this effect becomes less pronounced when considering the final corrosion rate. This reduction is likely due to the eventual formation of a protective FeS film. Further investigation emphasizes the significant impact of flow rate on corrosion, attributed to a combination of electrochemical factors and mechanical effects arising from fluid movement. Higher flow rates are closely associated with increased turbulence, which promotes the mixing of solutions and affects the corrosion rate of exposed steel surfaces [79]. Zhang et al. [80] investigated the corrosion rate of L360QS steel under flow rate, providing insights into the effect of flow rate on H2S corrosion. Corrosion rates remain relatively low at flow rates of 3-6 m/s. However, a significant increase occurs from 0.0132 to 0.1407 mm/a

(approximately 10 times) at flow rates of 6-8 m/s, respectively. Notably, higher corrosion rates are observed at lower water flow rates due to inadequate fluid power, resulting in ineffective removal of sulfur particles and severe corrosion. Conversely, mechanical erosion accelerates the removal of corrosion inhibitors and scales at higher flow speeds, worsening metal corrosion. Increased turbulence also affects the precipitation rate of $FeCO_3$. Before any film formation, high velocities lead to a higher corrosion rate. Turbulent flow facilitates the migration of cathodic species toward the steel surface while simultaneously expediting the transportation of Fe^{2+} ions away from the surface. Consequently, this dual effect reduces the concentration of Fe^{2+} ions at the steel surface, resulting in surface supersaturation and a decrease in the precipitation rate. The implications of flow rate on H2S corrosion are illustrated in Fig. 7.

4.3. Effect of H2S concentration

The concentration of H_2S plays a critical role in determining the susceptibility of various steel alloys to corrosion. In environments with consistent pH levels, increased H_2S concentrations result in decreased elongation and strength, indicating heightened susceptibility to corrosion. This effect is mainly attributed to the corrosive nature of H_2S [86]. Furthermore, H_2S concentration directly impacts the corrosion rate of carbon steel, with higher concentrations corresponding to increased corrosion levels. demonstrated a significant increase in the corrosion rates of carbon steel with higher H_2S concentrations in the solution. When the solution contained 408.44 mg/L of H_2S, the corrosion rate reached 19.06 g m^{-2} h^{-1}, nearly 13 times greater than the rate observed in a solution without H_2S (approximately 1.50 g m^{-2} h^{-1}). These findings emphasize the significant impact of elevated H_2S concentration on corrosion rates in solutions [87]. The enhanced corrosion is linked to the amplification of the hydrogen evolution reaction. Additionally, the formation of the initial mackinawite film is dependent on the H_2S concentration. In environments with low H_2S concentrations, primary corrosion products include mackinawite and cubic FeS [26]. Notably, the stability of the initial mackinawite film deteriorates when H_2S concentrations reach up

to 0.035 mol/L, causing film breakdown and increased susceptibility of carbon steel to localized corrosion and pitting [88]. On the other hand, in environments with high H_2S concentrations, main corrosion products shift to troilite and pyrrhotite, with some researchers also observing pyrite formation. Increased H_2S concentrations intensify the severity and rate of corrosion, fostering a more aggressive metal surface environment and accelerating the generation of corrosive species [89]. Fig. 7 provides a visual summary of the significant parameters affecting H_2S corrosion.

5. Monitoring

Effective management of H_2S in refineries is crucial due to its highly corrosive nature. Neglecting this issue can result in leaks, compromise equipment's structural integrity, and pose significant hazards. Continuous monitoring and the use of corrosion inhibitors are essential for mitigating potential risks associated with H_2S-induced corrosion. This proactive approach not only extends equipment lifespan but also enhances safety while reducing financial burdens related to corrosion-induced incidents. In refineries, addressing H_2S-induced corrosion requires a well-structured approach. The corrosion monitoring program involves several vital steps: H_2S detection, environmental and process monitoring, material selection, corrosion testing, inspection and maintenance protocols, corrosion inhibitor monitoring, and rigorous data analysis and reporting. Fostering a culture of training and awareness among personnel further strengthens defenses against H_2S corrosion risks. By implementing this integrated monitoring and preventive strategy, refineries can proactively safeguard their operations against H_2S-induced corrosion, ensuring reliability, longevity, and adherence to safety standards.

- Continuous monitoring

Continuous monitoring of H_2S using gas sensors in critical refinery areas is essential for promptly detecting potential risks. Implementing alarms and automatic shutdown systems for increased H_2S levels enhances safety, ensuring a swift response and minimizing hazards [90]. Deploying corrosion probes, coupons, or ultrasonic

thickness gauges effectively evaluates corrosion rates on metal surfaces exposed to H_2S-containing environments. Regular inspections and data analyses help identify potential corrosion hotspots. Monitoring process parameters such as pH, flow rates, pressure, and temperature are crucial, as they influence the severity of H_2S corrosion. Tracking process changes or upsets that may elevate H_2S concentration or alter the corrosion environment ensures a comprehensive approach to H_2S corrosion monitoring and mitigation in refinery settings [91]. Regular inspections are vital for detecting early signs of corrosion, such as pitting, scaling, or cracking in equipment exposed to H_2S-containing environments. Timely intervention prevents further deterioration and mitigates potential risks. Scheduled preventive maintenance and regular cleaning remove accumulated corrosion products, ensuring optimal performance and extending the service life of critical assets. Adherence to these protocols effectively safeguards infrastructure from H_2S-induced corrosion, enhances safety measures, and maintains operational integrity [92].

- Corrosion coatings

Protective coatings play a significant role in the oil and gas industry for mitigating corrosion problems, particularly those caused by H_2S in refinery operations. These coatings serve as a preventive measure by forming a barrier between metal surfaces and corrosive substances such as H_2S, reducing corrosion rates, and improving the lifespan and safety of equipment. They offer defense against various degradation mechanisms, including heat, erosion, pitting, and general wear [93,94]. Coatings are generally categorized into three main groups based on their material: organic, inorganic, and metallic. In refinery environments, all three types are used to protect equipment like tanks, pipes, and columns from the harmful effects of natural gas, water, and environmental factors. Recent advancements in coating technology have led to specialized formulations tailored for the oil and gas industry, optimizing refinery processes [95]. Commonly used coating systems include the three-layer polyolefin (3LPO) and fusion-bonded epoxy (FBE). A high-performance composite coating (HPCC) has been developed as a single-layer, powder-coated composite system. This

HPCC includes an FBE base coat, a medium-density polyethylene outer layer, and a tie layer made with chemically modified polyethylene adhesive. Each layer is applied via an electrostatic powder coating process, with the tie layer containing varying concentrations of FBE. This system provides exceptional adhesion, shear resistance, flexibility at low temperatures, impact and cathodic disbondment resistance to H_2S, and minimal moisture permeability, making it highly effective in protecting various types of steel in crude oil environments [94].

- Cathodic protection

Cathodic protection (CP) is crucial in combating corrosion in the oil and gas industry, especially in areas where H_2S poses significant risks to buried pipelines and storage facilities [94]. CP works by converting metal surfaces into cathodes within an electrochemical system, aiming to prevent stress corrosion cracking and reduce defects that can occur during the application and operational life of organic coatings, which are the primary methods for managing corrosion [95]. Combining CP with coatings is often considered the most cost-effective approach for corrosion prevention in refinery environments. CP aims to reduce corrosion by minimizing the potential difference between the anode and cathode. This is accomplished by applying an external current, such as to a pipeline, on the structure being protected. Providing sufficient current ensures the entire structure attains a uniform potential, effectively eliminating separate anode and cathode areas. This method is typically used alongside coatings [96]. Aboveground storage tanks often undergo CP on internal and external surfaces in refinery operations. While pure hydrocarbon fluids are generally non-corrosive, internal tank corrosion can occur in areas exposed to sediments, water, and other contaminants [94]. Effective CP operation requires all four fundamental components-anode, cathode, electrolyte, and a complete electrical circuit to ensure continuous corrosion protection against H2S. Although corrosion rates of metal structures under CP never reach zero, they are kept extremely low, reducing the risk of corrosion-induced failures [95]. The two main types of cathodic protection (CP) systems commonly employed are sacrificial (or galvanic) anode cathodic protection (SACP)

and impressed current cathodic protection (ICCP) [94,96]. SACP involves attaching active metals such as aluminum, zinc, or magnesium to the structure, which sacrificially corrode to protect the metal substrate from H_2S corrosion [95]. ICCP uses an external power source to supply current through inert or low-consumption-rate anodes, which are typically made of materials such as graphite, mixed metal oxides, or high-silicon cast iron [94]. To improve efficiency and lower costs, these anodes are often surrounded by carbonaceous backfill. Both SACP and ICCP provide effective corrosion protection for various metals and alloys commonly found in refinery infrastructure, including carbon steel, ductile iron, stainless steel, and aluminum [95].

- Material selection

Materials used in acid oil and gas operations primarily consist of carbon steels. However, the use of corrosion-resistant alloys (CRAs) for major equipment parts has been increasing due to advancements in CRAs and their improving economics. Selecting the right material is crucial for preventing expensive corrosion-related failures and ensuring the safety and reliability of industrial equipment and infrastructure. Materials that resist corrosion from H_2S are particularly important for maintaining the integrity and longevity of equipment and structures in H_2S-containing environments. Some materials recognized for their H_2S corrosion resistance include stainless steel, nickel-based alloys, titanium, duplex stainless steels (DSSs), high-density polyethylene, and fiber-reinforced polymers. Austenitic stainless steels are resistant to H_2S corrosion because of their high chromium content, which leads to the formation of a protective passive layer on the surface [98]. DSS, such as 2205, combines properties of both austenite and ferrite, offering excellent resistance to stress and H_2S corrosion [99]. These steels are highly valued for their strength, toughness, and corrosion resistance, serving as a cost-effective alternative to expensive nickel-based alloys and austenitic stainless steel. The superior corrosion resistance of DSS can be attributed to the formation of a protective passive film and the synergistic effects of their duplex microstructure. In 2205 DSS, this passive film exhibits heterogeneity, with molybdenum and chromium concentrated in the ferrite phase and nitrogen and

nickel in the austenite phase [100]. In H_2S-containing environments, the risk of pitting corrosion is increased compared to environments with CO_2. Studies indicate that pitting corrosion tends to be more severe on the ferrite phase than on the austenite phase in 2205 DSS samples exposed to H_2S-containing environments [101]. Some researchers suggest that the corrosion mechanism of 2205 DSS in H_2S environments differs from that in CO_2 environments due to the role of H_2S in accelerating the dissolution of the passive film and producing corrosion products. Furthermore, it has been observed that 22%Cr DSS can be safely used in environments with high concentrations of H_2S, indicating its suitability for such conditions [100]. Titanium and its alloys demonstrate excellent resistance to H_2S-induced corrosion, particularly in acidic environments. This is due to the formation of a protective surface layer made of TiO_2 in various corrosive settings [102]. In a study by Thorhallsson and Karlsdottir (2021) [102], a simulated high-temperature geothermal environment was used, ranging from 180 to 350 °C, with a gauge pressure of 10 bars. This environment consisted of gases like HCl, H_2S, and CO_2, along with an acidic condensate having a pH of 3. A specific titanium alloy, Ti-0.4Ni-3.6Mo-0.75Zr (Ti-475), showed remarkable corrosion resistance under these conditions, even when exposed to single superheated or two-phase conditions. This suggests that Ti-475 is a promising material for corrosion-prone environments. In another research effort, Ti-475 displayed outstanding corrosion resistance in simulated high-temperature geothermal conditions [103]. It showed no signs of corrosion when subjected to either single-superheated or two-phase states of the testing fluid. This remarkable resistance makes Ti-475 a suitable choice for applications where corrosion resistance is essential, especially in highly corrosive environments. The consistent performance of this alloy under such conditions establishes it as a reliable option for materials requiring high corrosion resistance. Nickel-based alloys are known for their excellent corrosion resistance in H_2S-containing environments, making them suitable for various applications in the petroleum and natural gas industries [104]. Generally, nickel-based alloys exhibit slightly better corrosion resistance than austenitic stainless steels, while austenitic stainless steels have significantly greater corrosion resistance

than ferritic/martensitic steels. The oil and gas industry values nickel-based alloys for their superior corrosion resistance and strength. However, structural changes during solidification may result in solidification cracks and reduced corrosion resistance. Additionally, these alloys may be susceptible to HE in hydrogen-containing environments, as observed in real-world conditions [81]. Alloy 625 stands out among these alloys due to its outstanding corrosion resistance and mechanical properties [105]. Alloy 625, a nickel–chromium alloy solid solution strengthened by molybdenum and niobium, is a prominent commercial grade. Its corrosion behavior in H_2S environments is influenced by its high alloy content, mainly nickel, chromium, and molybdenum. While these elements contribute to forming a dense, corrosion-resistant passive film in air, they can also lead to the development of specific microstructures called Laves and G phases. These intermetallic compounds may have different electrochemical properties than the surrounding matrix, making them more susceptible to preferential corrosion. In H_2S media, if the passive film breaks down, these distinct phases can accelerate localized corrosion, including pitting corrosion. This is particularly significant when combined with the galvanic mechanism, which involves a significant potential difference between the cathodic (matrix) and anodic (precipitates) regions. The occurrence of Laves and G phases increases the corrosion tendencies of Inconel 625 in H_2S environments [106].

Steel mills have created alloys with reduced levels of nickel and molybdenum to offer a stronger alternative to commonly used austenitic stainless steels like 304L and 316L. Molybdenum improves corrosion resistance by increasing the concentration of molybdenum and chromium in the protective film, resulting in a thicker film and a more stable chromium oxide layer. Molybdenum also hinders corrosion through mechanisms such as adsorption, compound formation, and interaction with other oxides [107]. A study by Tomio et al. [108] examined alloys with varying molybdenum levels for their susceptibility to SCC in an H_2S environment. The results showed that alloys with lower molybdenum content (<8%) were more susceptible to SCC, while those with higher molybdenum content (8–16%) exhibited greater resistance to SCC.

Microscopic examination of fracture surfaces confirmed molybdenum's protective role against SCC in this corrosive environment. The absence of molybdenum also led to pitting corrosion, suggesting a different form of corrosion. Copper-nickel alloys are widely used in seawater systems due to their high resistance to H_2S corrosion [109]. These alloys offer excellent corrosion resistance, machinability, high thermal and electrical conductivity, and moderate resistance to biological scaling. While copper alloys such as brass are widely used across industries, they can be susceptible to SCC, leading to cracks under pressure in damp conditions. Brass pipelines are particularly vulnerable to corrosion-induced cracking in sulfide-rich environments [110]. Brass alloys with high zinc content are prone to intergranular SCC in the presence of H_2S. For example, $CuZn_{37}$ and $CuZn_{20}Al_2$ are two distinct brass alloys suitable for the oil and gas industry. $CuZn_{37}$ has lower resistance to H_2S corrosion, making it less suitable for H_2S-containing environments. In contrast, $CuZn_{20}Al_2$ offers enhanced corrosion resistance to H_2S due to the inclusion of aluminum, making it a more suitable option for H_2S-exposed environments. The specific suitability of these alloys may also depend on temperature, pressure, and other environmental factors. High-density polyethylene (HDPE) is a corrosion-resistant polymer frequently used in pipeline applications to transport H_2S-containing fluids [111]. Fiber-reinforced polymers such as fiberglass composites exhibit good corrosion resistance and are suitable for various applications like tanks and structural components [112].

- Data analysis and reporting

Data analysis and reporting are critical components in managing H_2S-induced corrosion. By examining data collected from various monitoring systems, industries can gain valuable insights into the corrosion process, identify potential corrosion hotspots, and assess the effectiveness of corrosion control strategies. This systematic analysis enables informed decision-making regarding the performance of corrosion inhibitors, equipment conditions, and the need for maintenance and preventive actions. Advanced analytical methods, such as predictive modeling and machine learning, help in identifying subtle corrosion patterns, facilitating proactive corrosion control

measures. Enhanced data visualization tools also aid in presenting complex corrosion data in a user-friendly format, speeding up decision-making processes. This analysis helps in recognizing current corrosion trends and anticipating future risks, empowering industries to take proactive steps to minimize significant damage or downtime due to corrosion-related issues [113,114].

- Training

Training and awareness are essential aspects of managing H2S-induced corrosion. Proper training programs ensure that personnel working in H2S-exposed environments understand the corrosion risks and have the necessary knowledge and skills to implement appropriate corrosion control measures. By promoting awareness, industries can cultivate a proactive and safety-oriented workforce, thereby preventing corrosion-related incidents. Regular training sessions led by experienced professionals help keep the team updated on the latest corrosion mitigation techniques and advanced technologies for early detection. Encouraging active participation in safety protocols and establishing open communication channels for reporting corrosion concerns foster a culture of vigilance. Periodic emergency response drills ensure preparedness and promote a collaborative environment that values the contributions of all team members, thus promoting shared responsibility for corrosion control and safety measures [115].

- Corrosion inhibitor monitoring

Corrosion inhibitor monitoring is essential for protecting metal surfaces from H2S-induced corrosion. Organic inhibitors dominate the market at nearly 70% usage [97]. They're administered via continuous injection (10-1000 ppm) or batch treatment (1-20% vol). Effective inhibitors in acidic environments include polymer-based, Gemini-surfactant-based, imidazoline-based, and amine-based types [10]. Regular monitoring enables precise dosage adjustments, optimizing protection and extending equipment lifespan while providing cost-effective corrosion control.

6. Corrosion inhibitors

The corrosion inhibitor market has seen substantial growth, with organic corrosion inhibitors accounting for nearly 70% of the market share. According to the US industry forecast for 2017 and 2022, the demand for corrosion inhibitors was projected to grow at an annual rate of 4.1%, reaching a volume demand of 1.7 billion pounds. The market is marked by ongoing product innovation driven by research and development, with key players including Ashland, AkzoNobel, BASF SE, GE Water and Process Technologies, DuPont, Champion Technology Services, Renewable Lubricants, Ecolab, Cytec Industries, Cortec Corporation, and Lubrizol Corporation. Metal corrosion inhibitors can be administered through either injection or batch treatment techniques. For continuous injection, inhibitor concentrations typically range from 10 to 1000 ppm, whereas batch treatment methods necessitate concentrations between 1 and 20 vol%. The major reported inhibitors for sour environments can be divided into four types: amine-based, imidazoline-based, gemini surfactant-based, and water-soluble polymer-based. Corrosion inhibitors can also be classified as cathodic, anodic, or mixed, depending on their influence on retarding the cathodic or anodic reaction of the corrosion process, or both. They can be further categorized as organic, inorganic, and hybrid (organic/inorganic) materials, as well as cathodic, anodic, and/or mixed-type inhibitors based on the active inhibitor molecules that impede the corrosion process.

Amines are the most extensively utilized organic compounds as sour corrosion inhibitors, garnering approximately 40% of research attention. As cost-effective, film-forming inhibitors, they are more affordable than other organic inhibitors like imidazolines and amides. Amine-based inhibitors demonstrate high corrosion inhibition efficiency due to the nitrogen heteroatom, which possesses high electron density, acting as the adsorption center. Sour corrosion inhibition by amines occurs through chemical adsorption where the electron pair on the nitrogen atom is transferred to the empty orbital of an iron atom. The extent of chemical interaction depends on the strength of amine-metal bonds. Fig. 8 showcases the chemical structures of some potent

sour corrosion inhibitors based on amine chemistry [116].

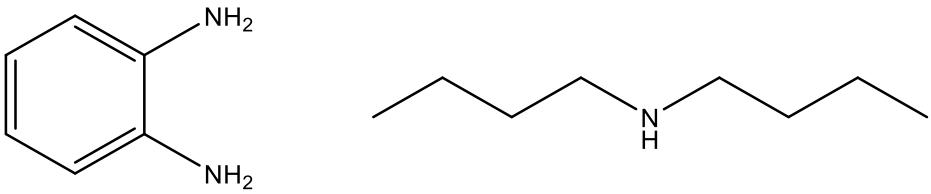

Fig. 8. Chemical structures of some potent amine-based sour corrosion inhibitors

Imidazolines, like amines, contain nitrogen but differ structurally, , featuring two nitrogen atoms within a heterocyclic ring. These nitrogen atoms occupy three unique bonding positions: pyridine-like N3, pyrrole-like N1, and aromatic ring nitrogen atoms. Imidazolines are found in three isomeric forms: 2-imidazoline, 3-imidazoline, and 4-imidazoline, with 2-imidazoline being the most prevalent. Beyond their chemical properties, 2-imidazoline is also utilized for its therapeutic effects, serving as an antihyperglycemic, anti-inflammatory, antihypertensive, antihypercholesterolemic, and antidepressant agent. Imidazolines and their derivatives, second only to amines, are the most studied sour corrosion inhibitors and represent the prevailing chemistry in this field. Imidazolines are considered negatively charged cationic surfactants unaffected by pH changes. They exhibit excellent corrosion inhibition properties in sour environments. The chemical structure of typical imidazoline-based inhibitor is shown in Fig. 9 [116]. The mechanism of sour corrosion inhibition by imidazolines is debated. One proposed theory indicates that inhibition primarily results from the imidazoline ring bonding to the metal surface in a planar configuration. In this process, the hydrophobic segment of the molecule plays a significant role, whereas the influence of the pendant group is relatively minor. Another perspective posits that the mechanism involves a combination of blocking, activation, and energy-related factors. Another perspective suggests that inhibition occurs through the creation of a self-assembled monolayer on the metal's native oxide surface, which acts as a hydrophobic barrier to prevent the penetration of corrosive species. For this monolayer to form effectively, the imidazoline molecule must include a hydrocarbon tail with a minimum of 12 carbon atoms. Additionally, the combination of the tail and the hydrophilic head must yield an

octanol/water partition coefficient that falls below a specific critical threshold.

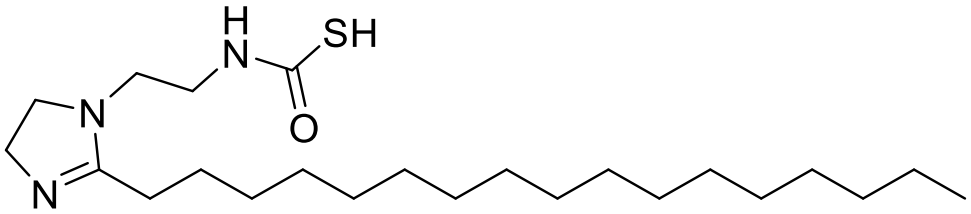

Fig. 9. Chemical structure of typical imidazoline-based sour corrosion inhibitor

Gemini cationic surfactants are synthetic amphiphilic molecules that consist of at least two hydrophilic head groups and two hydrophobic tails, linked by a spacer located near the head groups. The spacer can vary in nature, being either hydrophobic or hydrophilic, and rigid or flexible. In comparison to traditional monomeric surfactants, gemini surfactants demonstrate several advantageous properties, such as lower critical micelle concentrations, superior wetting capabilities, reduced limiting surface tensions, and unique aggregation behaviors. These surfactants also exhibit a broad range of hydrophilic-lipophilic balance (HLB), which influences their water solubility. This versatility makes gemini surfactants highly suitable for a variety of applications, including detergents, cosmetics, personal care products, paint and coating additives, biocides, material science, organic synthesis, pharmaceuticals, textiles, enhanced oil recovery, nanotechnology, petroleum, and more. As sour corrosion inhibitors, gemini surfactants have received about 25% of research attention. They are often used as quaternized salts to prevent the formation of imino or amido moieties, which are believed to have little to no corrosion inhibition properties. Examples of gemini surfactants reported in corrosion literature as sour corrosion inhibitors are provided in Fig. 10 [116]. Gemini surfactants inhibit corrosion by adsorbing the polar group (hydrophilic head) to the metal surface, while orienting the non-polar group (hydrophobic tail) outward toward the solution.

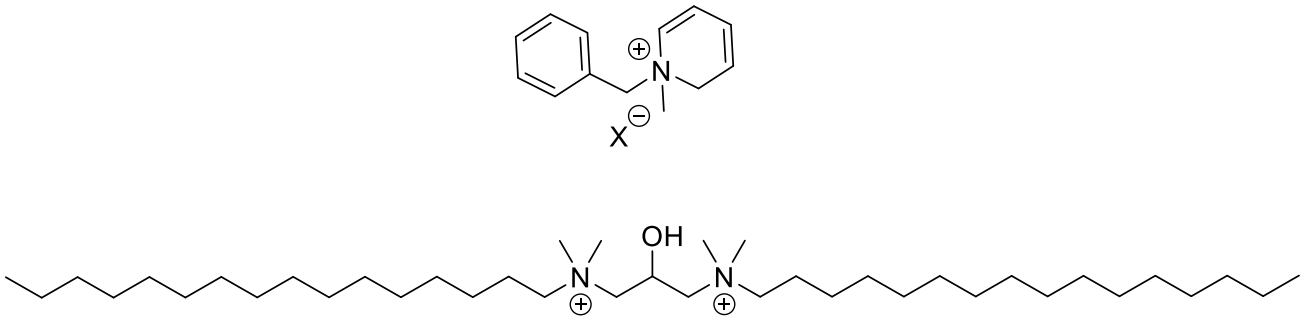

Fig. 10. Chemical structures of sour corrosion inhibitors based on gemini surfactant

Acrylic terpolymers, derived from three distinct monomers, have been reported as effective sour corrosion inhibitors. With 0.8 mmol/l of terpolymer and a rotation speed of 2000 rpm, inhibition efficiency above 90% was achieved. However, polymer-based inhibitors have received the least attention (about 6%) compared to other classes of sour corrosion inhibitors. This lack of attention may be due to the poor solubility of polymers in aqueous solutions, often resulting in moderate corrosion inhibition under static conditions. Additionally, polymers are unstable at high temperatures, limiting their use in environments exceeding 120 °C. Nonetheless, modification approaches like copolymerization, synergistic combinations with other substances, cross-linking, and compositing have been employed to enhance corrosion inhibition.

Single compounds often fail to provide adequate corrosion protection for metallic substrates in corrosive environments. Ideally, the corrosion rate of carbon steel in such environments should not exceed 4 mpy. Commercial corrosion inhibitors are formulations containing an active compound, co-active, intensifier, surfactant, solvent, and co-solvent. Some formulations may also include anti-foaming and anti-wetting agents. Most sour corrosion inhibitor cocktails utilize amines, imidazolines, gemini surfactants, or polymers as the primary active components. Common corrosion inhibitor intensifiers include potassium iodide, methyl formate, copper iodide, copper chloride, and metal cations (Zn^{2+}, As^{3+}, Cr^{3+}, Cu^{2+}, Ni^{2+}, and Sn^{2+}). These intensifiers enhance the performance of the primary active component, ensuring effective corrosion inhibition.

7. Evaluation methods of corrosion inhibitors

There are several methods employed to evaluate the performance and efficiency of corrosion inhibitors. These methods can be broadly classified into laboratory tests and field tests.

Laboratory Tests:

1. **Weight Loss Method:** This method follows the ASTM G31-72 standard. A pre-weighed metal specimen is immersed in a corrosive solution, both with and without the corrosion inhibitor. After a specified time, the specimens are removed, cleaned, and re-weighed. The difference in weight loss between the inhibited and uninhibited specimens is used to calculate the inhibition efficiency using the formula (1):

$$\eta = \frac{W_0 - W_1}{W_0} * 100\% \quad (1)$$

where η = inhibition efficiency, W_o = weight loss without inhibitor, and W_i = weight loss with inhibitor.

2. **Electrochemical Techniques:** These techniques involve measuring various electrochemical parameters: Potentiodynamic Polarization: This method follows ASTM G5-94 and involves measuring the corrosion potential (E_o), corrosion current (i_o), and anodic/cathodic Tafel slopes. The inhibition efficiency is calculated using the formula (2):

$$\eta = \frac{I_{00} - I_{0i}}{I_{00}} * 100\% \quad (2)$$

where η = inhibition efficiency, i_{oo} = corrosion current without inhibitor, and i_{oi} = corrosion current with inhibitor.

3. **Electrochemical Impedance Spectroscopy (EIS):** This method follows

ASTM G106-89 and measures the impedance of a metal-electrolyte interface at various frequencies. The inhibition efficiency is calculated from the difference in charge transfer resistance (R_p) with and without the inhibitor (3):

$$\eta = \frac{R_{p0} - R_{pi}}{R_{p0}} * 100\% \quad (3)$$

where η = inhibition efficiency, R_{p0} = charge transfer resistance without inhibitor, and R_{pi} = charge transfer resistance with inhibitor.

Surface Analysis Techniques:

Scanning Electron Microscopy (SEM): SEM provides high-resolution images of the metal surface at the micron and nanometer scale, revealing surface morphology and inhibitor adsorption behavior.

Energy-Dispersive X-ray Spectroscopy (EDS): EDS provides elemental composition analysis of the metal surface, helping to determine the presence of the inhibitor elements.

Atomic Force Microscopy (AFM): AFM offers 3D surface topography and roughness analysis, providing insights into inhibitor adsorption and surface interaction.

Field Tests:

Coupon Tests: Coupons made of the metal being studied are exposed to the corrosive environment with and without the inhibitor. The corrosion rates and inhibition efficiency are determined by measuring the weight loss of the coupons after a specified time.

Electrical Resistance (ER) Probes: ER probes follow the ASTM G96-90 standard and involve measuring the electrical resistance of a metal element exposed to the corrosive environment. The corrosion rate and inhibition efficiency can be monitored in real-time by tracking changes in resistance.

Linear Polarization Resistance (LPR): The LPR technique follows ASTM G96-90 and involves applying a small potential perturbation to the metal surface while

measuring the resulting current response. The corrosion rate and inhibition efficiency can be calculated from the polarization resistance (R_p).

Harmonic Analysis: This method involves applying a sinusoidal voltage to the metal surface and measuring the resulting current response. The phase shift and amplitude of the current signal can be used to determine the corrosion rate and inhibition efficiency.

These methods enable researchers and engineers to determine the effectiveness of corrosion inhibitors under various conditions and help in selecting the most suitable inhibitor for a particular application.

Conclusion

Addressing H_2S corrosion in the oil and gas industry necessitates a well-defined and integrated strategy. Comprehending corrosion mechanisms such as HIC, SOHIC, SSC, HE, and is essential for pinpointing contributing factors and establishing a proactive strategy.

Tools for preventive corrosion monitoring, like ultrasonic gauges and gas sensors, are critical for identifying issues early and reducing risks. Material selection is crucial, focusing on stainless steel, nickel-based alloys, and copper-nickel alloys to combat H_2S-induced corrosion. Monitoring and adjusting corrosion inhibitors are necessary for optimal protection. Data analysis provides insights into corrosion patterns, supporting informed decision-making processes.

A comprehensive corrosion control strategy involves routine inspections, preventive maintenance, and ongoing workforce training. Integrating material science, corrosion engineering, and advanced monitoring technologies is vital for protecting assets and minimizing H_2S-induced corrosion risks in the oil and gas sector.

A major challenge for sour corrosion inhibitors worldwide is their non-compliance with environmental regulations. While green substances, such as natural polymers, are more eco-friendly, they are less effective in combating corrosion caused by acidic gases. Future research should focus on exploring innovative organic compounds in the categories of amino acids, plant extracts, and ionic liquids (ILs). Polyaspartic acid, lactobionic acid, polysuccinimide, and their derivatives have demonstrated excellent corrosion inhibition properties.

Plant-based extracts offer cost-effective and eco-friendly alternatives. For instance, 2.7 g/l lemon verbena extract was found to protect carbon steel by 95.61% in H_2S-containing environments. Similarly, ILs are also environmentally friendly and have shown effectiveness in retarding corrosion in various corrosive media. The development of corrosion inhibitors that are both effective and compliant with environmental regulations remains an important area of ongoing research.

Advancements in managing H_2S corrosion are anticipated. Future perspectives

include the integration of advanced technologies, such as real-time monitoring through sensors, to expedite accurate corrosion detection. Ongoing research may lead to more resilient alloys and sustainable corrosion inhibitors tailored for H_2S-exposed environments.

International collaborations will play a crucial role in fostering global understanding, and continuous workforce training is essential for staying updated with the latest technologies and best practices. The future outlook involves a dynamic blend of technological innovation, material science advancements, and collaborative efforts to ensure the integrity and safety of oil and gas infrastructure amidst evolving challenges.

References

1. Fanun M. (ed.). The role of colloidal systems in environmental protection. – Elsevier, 2014.
2. Soomro A. A. et al. Integrity assessment of corroded oil and gas pipelines using machine learning: A systematic review //Engineering Failure Analysis. – 2022. – T. 131. – C. 105810.
3. Senouci A. et al. A model for predicting failure of oil pipelines //Structure and Infrastructure Engineering. – 2014. – T. 10. – №. 3. – C. 375-387.
4. Vakili M., Koutník P., Kohout J. Addressing Hydrogen Sulfide Corrosion in Oil and Gas Industries: A Sustainable Perspective //Sustainability. – 2024. – T. 16. – №. 4. – C. 1661.
5. Obot I. B. et al. Key parameters affecting sweet and sour corrosion: Impact on corrosion risk assessment and inhibition //Engineering Failure Analysis. – 2023. – T. 145. – C. 107008.
6. Song C. et al. Failure analysis of the crack and leakage of a crude oil pipeline under CO2-steam flooding //Processes. – 2023. – T. 11. – №. 5. – C. 1567.
7. Zhao W. et al. Corrosion failure mechanism of associated gas transmission pipeline //Materials. – 2018. – T. 11. – №. 10. – C. 1935.
8. Shi X. et al. Corrosion law of metal pipeline in tahe oilfield and application of new materials //Coatings. – 2021. – T. 11. – №. 11. – C. 1269.
9. Videm K., Koren A. M. Corrosion, passivity, and pitting of carbon steel in aqueous solutions of HCO3−, CO2, and Cl− //Corrosion. – 1993. – T. 49. – №. 9. – C. 746-754.
10. Obot I. B. et al. Progress in the development of sour corrosion inhibitors: Past, present, and future perspectives //Journal of Industrial and Engineering Chemistry. – 2019. – T. 79. – C. 1-18.
11. Guidotti T. L. Hydrogen sulfide intoxication //Handbook of clinical neurology. – Elsevier, 2015. – T. 131. – C. 111-133.
12. Ausma T., De Kok L. J. Atmospheric H2S: impact on plant functioning //Frontiers in Plant Science. – 2019. – T. 10. – C. 743.
13. Ahmad W. et al. A review on the removal of hydrogen sulfide from biogas by adsorption using sorbents derived from waste //Reviews in Chemical Engineering. – 2021. – T. 37. – №. 3. – C. 407-431.
14. Kraia T. et al. Unveiling the role of in situ sulfidation and H2O excess on H2S decomposition to carbon-free H2 over cobalt/ceria catalysts //Catalysts. – 2023. – T. 13. – №. 3. – C. 504.
15. Costa C. et al. Hydrogen sulfide adsorption by iron oxides and their polymer composites: a case-study application to biogas purification //Materials. – 2020. – T. 13. – №. 21. – C. 4725.
16. Afzal S. et al. Catalytic hydrogen evolution from H2S cracking over CrxZnS Catalyst in a cylindrical single-layered dielectric barrier discharge plasma reactor //Materials. – 2022. – T. 15. – №. 21. – C. 7426.
17. Tian R. et al. Energy consumption analysis of a diesel hydrotreating unit using an aspen simulation //Processes. – 2022. – T. 10. – №. 10. – C. 2055.
18. Magomedov R. N. et al. Current status and prospects of demetallization of heavy petroleum feedstock //Petroleum Chemistry. – 2015. – T. 55. – C. 423-443.
19. Jagannath A., Ibrahim S., Raj A. Heat Integration in Straight-Through Sulfur Recovery Units to Increase Net High-Pressure Steam Production //Chemical Engineering & Technology. – 2021. – T. 44. – №. 1. – C. 164-173.
20. Salah H. B., Nancarrow P., Al-Othman A. Ionic liquid-assisted refinery processes–A review and industrial perspective //Fuel. – 2021. – T. 302. – C. 121195.
21. Yang R. et al. Cause analysis and prevention measures of fire and explosion caused by sulfur corrosion //Engineering failure analysis. – 2020. – T. 108. – C. 104342.
22. Jiad M. M., Abbar A. H. Petroleum refinery wastewater treatment using a novel combined electro-Fenton and photocatalytic process //Journal of Industrial and Engineering Chemistry. – 2024. – T. 129. – C. 634-655.
23. Asadian M., Sabzi M., Anijdan S. H. M. The effect of temperature, CO2, H2S gases and the resultant iron carbonate and iron sulfide compounds on the sour corrosion behaviour of ASTM A-106 steel for pipeline transportation //International Journal of Pressure Vessels and Piping. – 2019. – T. 171. – C. 184-193.
24. Liu W. et al. Investigation of corrosion sequence in the overhead pipeline of H2S stripper column through CFD models //Engineering Failure Analysis. – 2022. – T. 136. – C. 106187.
25. Lins V. F. C., Guimarães E. M. Failure of a heat exchanger generated by an excess of SO2 and H2S in the sulfur recovery unit of a petroleum refinery //Journal of Loss Prevention in the Process Industries.

– 2007. – Т. 20. – №. 1. – С. 91-97.

26. Zheng S. et al. Dependence of the abnormal protective property on the corrosion product film formed on H2S-adjacent API-X52 pipeline steel //International Journal of Hydrogen Energy. – 2014. – Т. 39. – №. 25. – С. 13919-13925.

27. Lucio-Garcia M. A. et al. Effect of heat treatment on H2S corrosion of a micro-alloyed C–Mn steel //Corrosion Science. – 2009. – Т. 51. – №. 10. – С. 2380-2386.

28. Shi F. et al. Polymorphous FeS corrosion products of pipeline steel under highly sour conditions //Corrosion Science. – 2016. – Т. 102. – С. 103-113.

29. Askari M., Aliofkhazraei M., Afroukhteh S. A comprehensive review on internal corrosion and cracking of oil and gas pipelines //Journal of Natural Gas Science and Engineering. – 2019. – Т. 71. – С. 102971.

30. Ohfuji H., Rickard D. High resolution transmission electron microscopic study of synthetic nanocrystalline mackinawite //Earth and Planetary Science Letters. – 2006. – Т. 241. – №. 1-2. – С. 227-233.

31. Boursiquot S. et al. The dry oxidation of tetragonal FeS 1-x mackinawite //Physics and Chemistry of Minerals. – 2001. – Т. 28. – С. 600-611.

32. Pearce C. I., Pattrick R. A. D., Vaughan D. J. Electrical and magnetic properties of sulfides //Reviews in Mineralogy and Geochemistry. – 2006. – Т. 61. – №. 1. – С. 127-180.

33. Davison W. The solubility of iron sulphides in synthetic and natural waters at ambient temperature //Aquatic Sciences. – 1991. – Т. 53. – С. 309-329.

34. El-Sherik A. M. (ed.). Trends in oil and gas corrosion research and technologies: Production and transmission. – Woodhead Publishing, 2017.

35. Wen X. et al. Review of recent progress in the study of corrosion products of steels in a hydrogen sulphide environment //Corrosion Science. – 2018. – Т. 139. – С. 124-140.

36. Ren C. et al. Corrosion behavior of oil tube steel in simulant solution with hydrogen sulfide and carbon dioxide //Materials chemistry and physics. – 2005. – Т. 93. – №. 2-3. – С. 305-309.

37. Skála R., Císařová I., Drábek M. Inversion twinning in troilite //American Mineralogist. – 2006. – Т. 91. – №. 5-6. – С. 917-921.

38. Wang H., Salveson I. A review on the mineral chemistry of the non-stoichiometric iron sulphide, Fe1− x S (0≤ x≤ 0.125): polymorphs, phase relations and transitions, electronic and magnetic structures //Phase Transitions. – 2005. – Т. 78. – №. 7-8. – С. 547-567.

39. Lefèvre C. T. et al. A cultured greigite-producing magnetotactic bacterium in a novel group of sulfate-reducing bacteria //Science. – 2011. – Т. 334. – №. 6063. – С. 1720-1723.

40. Kitchaev D. A., Ceder G. Evaluating structure selection in the hydrothermal growth of FeS2 pyrite and marcasite //Nature communications. – 2016. – Т. 7. – №. 1. – С. 13799.

41. Jeong H. Y., Lee J. H., Hayes K. F. Characterization of synthetic nanocrystalline mackinawite: crystal structure, particle size, and specific surface area //Geochimica et cosmochimica acta. – 2008. – Т. 72. – №. 2. – С. 493-505.

42. Ma H. Y. et al. Theoretical interpretation on impedance spectra for anodic iron dissolution in acidic solutions containing hydrogen sulfide //Corrosion. – 1998. – Т. 54. – №. 8. – С. 634-640.

43. Ma H. et al. The influence of hydrogen sulfide on corrosion of iron under different conditions //Corrosion science. – 2000. – Т. 42. – №. 10. – С. 1669-1683.

44. Vakili M., Koutník P., Kohout J. Addressing Hydrogen Sulfide Corrosion in Oil and Gas Industries: A Sustainable Perspective //Sustainability. – 2024. – Т. 16. – №. 4. – С. 1661.

45. Vakili M., Koutník P., Kohout J. Addressing Hydrogen Sulfide Corrosion in Oil and Gas Industries: A Sustainable Perspective //Sustainability. – 2024. – Т. 16. – №. 4. – С. 1661.

46. El-Sherik A. M. (ed.). Trends in oil and gas corrosion research and technologies: Production and transmission. – Woodhead Publishing, 2017.

47. Rickard D., Luther G. W. Chemistry of iron sulfides //Chemical reviews. – 2007. – Т. 107. – №. 2. – С. 514-562.

48. Ossai C. I., Boswell B., Davies I. J. Pipeline failures in corrosive environments–A conceptual analysis of trends and effects //Engineering Failure Analysis. – 2015. – Т. 53. – С. 36-58.

49. Anijdan S. H. M. et al. Sensitivity to hydrogen induced cracking, and corrosion performance of an API X65 pipeline steel in H2S containing environment: influence of heat treatment and its subsequent microstructural changes //journal of materials research and technology. – 2021. – Т. 15. – С. 1-16.

50. Abdelshafeek K. A. et al. Vicia faba peel extracts bearing fatty acids moieties as a cost-

effective and green corrosion inhibitor for mild steel in marine water: computational and electrochemical studies //Scientific Reports. – 2022. – Т. 12. – №. 1. – С. 20611.

51. Bertoncello J. C. B. et al. Effects of thermal spray aluminium coating on SSC and HIC resistance of high strength steel in a sour environment //Surface and Coatings Technology. – 2020. – Т. 399. – С. 126156.

52. Traidia A. et al. An effective finite element model for the prediction of hydrogen induced cracking in steel pipelines //International Journal of Hydrogen Energy. – 2012. – Т. 37. – №. 21. – С. 16214-16230.

53. Martin M. L., Sofronis P. Hydrogen-induced cracking and blistering in steels: A review //Journal of Natural Gas Science and Engineering. – 2022. – Т. 101. – С. 104547.

54. Campos E. S. et al. Influence of metallurgical factors on the hydrogen induced cracking of carbon steel wires in H2S-containing environments //Engineering Failure Analysis. – 2024. – Т. 155. – С. 107739.

55. Toribio J. et al. Residual stress redistribution induced by fatigue in cold-drawn prestressing steel wires //Construction and Building Materials. – 2016. – Т. 114. – С. 317-322.

56. De Giorgi M. Residual stress evolution in cold-rolled steels //International Journal of Fatigue. – 2011. – Т. 33. – №. 3. – С. 507-512.

57. Domizzi G., Anteri G., Ovejero-Garcıa J. Influence of sulphur content and inclusion distribution on the hydrogen induced blister cracking in pressure vessel and pipeline steels //Corrosion Science. – 2001. – Т. 43. – №. 2. – С. 325-339.

58. Mohtadi-Bonab M. A., Szpunar J. A., Razavi-Tousi S. S. A comparative study of hydrogen induced cracking behavior in API 5L X60 and X70 pipeline steels //Engineering Failure Analysis. – 2013. – Т. 33. – С. 163-175.

59. Lee H. L., Chan S. L. I. Hydrogen embrittlement of AISI 4130 steel with an alternate ferrite/pearlite banded structure //Materials Science and Engineering: A. – 1991. – Т. 142. – №. 2. – С. 193-201.

60. Tau L., Chan S. L. I. Effects of ferrite/pearlite alignment on the hydrogen permeation in a AISI 4130 steel //Materials Letters. – 1996. – Т. 29. – №. 1-3. – С. 143-147.

61. Roccisano A., Nafisi S., Ghomashchi R. Stress corrosion cracking observed in ex-service gas pipelines: A comprehensive study //Metallurgical and Materials Transactions A. – 2020. – Т. 51. – С. 167-188.

62. Wang Q. et al. Effect of niobium on sulfide stress cracking behavior of tempered martensitic steel //Corrosion Science. – 2020. – Т. 165. – С. 108387.

63. Zvirko O. et al. Assessment of in-service degradation of gas pipeline steel taking into account susceptibility to stress corrosion cracking //Procedia Structural Integrity. – 2019. – Т. 16. – С. 121-125.

64. Sherif E. S. M. et al. Corrosion and Corrosion Inhibition of High Strength Low Alloy Steel in 2.0 M Sulfuric Acid Solutions by 3-Amino-1, 2, 3-triazole as a Corrosion Inhibitor //Journal of Chemistry. – 2014. – Т. 2014. – №. 1. – С. 538794.

65. Seikh A. H., Sherif E. S. M. Effects of immersion time and temperature on the corrosion of API 5L Grade X-65 Steel in 1.0 M H2SO4 pickling solution //International Journal of Electrochemical Science. – 2015. – Т. 10. – №. 1. – С. 895-908.

66. Chong T. V. S. et al. Effects of wet H2S containing environment on mechanical properties of NACE grade C–Mn steel pipeline girth welds //Engineering Fracture Mechanics. – 2014. – Т. 131. – С. 485-503.

67. El-Shamy A. M. et al. Potential removal of organic loads from petroleum wastewater and its effect on the corrosion behavior of municipal networks //Journal of environmental management. – 2018. – Т. 219. – С. 325-331.

68. Suman S., Biswas P. Comparative study on SAW welding induced distortion and residual stresses of CSEF steel considering solid state phase transformation and preheating //Journal of Manufacturing Processes. – 2020. – Т. 51. – С. 19-30.

69. Haidemenopoulos G. N. et al. Investigation of stress-oriented hydrogen-induced cracking (SOHIC) in an amine absorber column of an oil refinery //Metals. – 2018. – Т. 8. – №. 9. – С. 663.

70. Al-Anezi M. A., Rao S. Failures by SOHIC in sour hydrocarbon service //Journal of failure analysis and prevention. – 2011. – Т. 11. – С. 363-371.

71. El-Shamy A. M. Fabrication of commercial nanoporous alumina by low voltage anodizing //Egyptian Journal of Chemistry. – 2018. – Т. 61. – №. 1. – С. 175-185.

72. Mohtadi-Bonab M. A. et al. Finite element modeling of HIC propagation in pipeline steel with regard to experimental observations //International Journal of Hydrogen Energy. – 2020. – Т. 45. – №. 43. – С. 23122-23133.
73. Wang Z., Feng Z., Zhang L. Effect of high temperature on the corrosion behavior and passive film composition of 316 L stainless steel in high H2S-containing environments //Corrosion Science. – 2020. – Т. 174. – С. 108844.
74. Medvedeva M. L. Specifics of high-temperature corrosion processes during oil recovery //Chemical and petroleum engineering. – 2000. – Т. 36. – №. 11. – С. 749-754.
75. Zhang L. et al. The corrosion behavior of 316L stainless steel in H2S environment at high temperatures //International Journal of Electrochemical Science. – 2017. – Т. 12. – №. 9. – С. 8806-8819.
76. Silva C. C., Farias J. P., de Sant'Ana H. B. Evaluation of AISI 316L stainless steel welded plates in heavy petroleum environment //Materials & Design. – 2009. – Т. 30. – №. 5. – С. 1581-1587.
77. Gao S. et al. Effect of high temperature on the aqueous H2S corrosion of mild steel //Corrosion. – 2017. – Т. 73. – №. 10. – С. 1188-1191.
78. Sun W., Nešic S., Papavinasam S. Kinetics of corrosion layer formation. Part 2—Iron sulfide and mixed iron sulfide/carbonate layers in carbon dioxide/hydrogen sulfide corrosion //Corrosion. – 2008. – Т. 64. – №. 7. – С. 586-599.
79. Asmara Y. P. The roles of H2S gas in behavior of carbon steel corrosion in oil and gas environment: a review //Jurnal Teknik Mesin (JTM). – 2018. – Т. 7. – №. 1. – С. 37-43.
80. Zhang N. et al. Effect of flow velocity on pipeline steel corrosion behaviour in H2S/CO2 environment with sulphur deposition //Corrosion Engineering, Science and Technology. – 2018. – Т. 53. – №. 5. – С. 370-377.
81. Martelo D. et al. Correlative analysis of digital imaging, acoustic emission, and fracture surface topography on hydrogen assisted cracking in Ni-alloy 625+ //Engineering Fracture Mechanics. – 2019. – Т. 221. – С. 106678.
82. Farhadian A. et al. Efficient dual-function inhibitors for prevention of gas hydrate formation and CO2/H2S corrosion inside oil and gas pipelines //Chemical Engineering Journal. – 2022. – Т. 431. – С. 134098.
83. Kermani M. B., Morshed A. Carbon dioxide corrosion in oil and gas productiona compendium //Corrosion. – 2003. – Т. 59. – №. 08.
84. Vakili M., Koutník P., Kohout J. Addressing Hydrogen Sulfide Corrosion in Oil and Gas Industries: A Sustainable Perspective //Sustainability. – 2024. – Т. 16. – №. 4. – С. 1661.
85. Brown B., Nešic S. Aspects of localized corrosion in an H2S/CO2 environment //Nace Corrosion. – NACE, 2012. – С. NACE-2012-1559.
86. Liu R. et al. Effect of pH and H2S concentration on sulfide stress corrosion cracking (SSCC) of API 2205 duplex stainless steel //International Journal of Materials Research. – 2021. – Т. 106. – №. 6. – С. 608-613.
87. Tang J. et al. The effect of H2S concentration on the corrosion behavior of carbon steel at 90 C //Corrosion Science. – 2010. – Т. 52. – №. 6. – С. 2050-2058.
88. Taheri H. et al. The effect of H2S concentration and temperature on corrosion behavior of pipeline steel A516-Gr70 //Caspian Journal of Applied Sciences Research. – 2012. – Т. 1. – №. 5. – С. 41-47.
89. Qi Y. et al. Effect of H2S partial pressure on the tensile properties of A350LF2 steel in the absence and presence of pre-immersion //Materials Science and Engineering: A. – 2014. – Т. 609. – С. 161-167.
90. Musayeva N. et al. Highly selective detection of hydrogen sulfide by simple Cu-CNTs nanocomposites //C. – 2023. – Т. 9. – №. 1. – С. 25.
91. Khalid H. U., Ismail M. C., Nosbi N. Permeation damage of polymer liner in oil and gas pipelines: A review //Polymers. – 2020. – Т. 12. – №. 10. – С. 2307.
92. Ali M. A. H. et al. An automatic visual inspection of oil tanks exterior surface using unmanned aerial vehicle with image processing and cascading fuzzy logic algorithms //Drones. – 2023. – Т. 7. – №. 2. – С. 133.
93. Cheng L., Lou F., Guo W. Corrosion protection of the potassium silicate conversion coating //Vacuum. – 2020. – Т. 176. – С. 109325.
94. Al-Moubaraki A. H., Obot I. B. Corrosion challenges in petroleum refinery operations: Sources, mechanisms, mitigation, and future outlook //Journal of Saudi Chemical Society. – 2021. – Т. 25. –

№. 12. – С. 101370.

95. Groysman A. Corrosion problems and solutions in oil, gas, refining and petrochemical industry //KOM–Corrosion and Material Protection Journal. – 2017. – Т. 61. – №. 3. – С. 100-117.

96. Popoola L. T. et al. Corrosion problems during oil and gas production and its mitigation //International Journal of Industrial Chemistry. – 2013. – Т. 4. – С. 1-15.

97. Umoren S. A., Solomon M. M., Saji V. S. Corrosion inhibitors for sour oilfield environment (H2S corrosion) //Corrosion Inhibitors in the Oil and Gas Industry. – 2020. – С. 229-254.

98. Zhao X. et al. Effect of CO2/H2S and applied stress on corrosion behavior of 15Cr tubing in oil field environment //Metals. – 2020. – Т. 10. – №. 3. – С. 409.

99. Dong C. et al. Effect of temperature and Cl− concentration on pitting of 2205 duplex stainless steel //Journal of Wuhan University of Technology-Mater. Sci. Ed. – 2011. – Т. 26. – С. 641-647.

100. Liu H. et al. Stability of passive film and pitting susceptibility of 2205 duplex stainless steel in CO2/H2S-containing geothermal environment //Corrosion Science. – 2023. – Т. 210. – С. 110832.

101. Zheng S. Q., Chen C. F., Chen L. Q. Corrosion characteristics of 2205 duplex stainless steel in high temperature and high pressure environment containing H2S/CO2 //Applied Mechanics and Materials. – 2012. – Т. 236. – С. 95-98.

102. Thorhallsson A. I., Karlsdottir S. N. Corrosion behaviour of titanium alloy and carbon steel in a high-temperature, single and mixed-phase, simulated geothermal environment containing H2S, CO2 and HCl //Corrosion and Materials Degradation. – 2021. – Т. 2. – №. 2. – С. 190-209.

103. Karlsdottir S. N. et al. Corrosion testing in superheated geothermal steam in Iceland //Geothermics. – 2015. – Т. 53. – С. 281-290.

104. Kang Y. et al. Review on the corrosion behaviour of nickel-based alloys in supercritical carbon dioxide under high temperature and pressure //Crystals. – 2023. – Т. 13. – №. 5. – С. 725.

105. Silva C. C. et al. New insight on the solidification path of an alloy 625 weld overlay //Journal of Materials research and Technology. – 2013. – Т. 2. – №. 3. – С. 228-237.

106. Guo Q. et al. Study of the pitting corrosion at welding joints of Inconel 625 alloy under high temperature and high H2S/CO2 partial pressure //International journal of electrochemical science. – 2017. – Т. 12. – №. 10. – С. 8929-8943.

107. Montemor M. F. et al. The role of Mo in the chemical composition and semiconductive behaviour of oxide films formed on stainless steels //Corrosion science. – 1999. – Т. 41. – №. 1. – С. 17-34.

108. Tomio A. et al. Role of alloyed molybdenum on corrosion resistance of austenitic Ni–Cr–Mo–Fe alloys in H2S–Cl–environments //Corrosion Science. – 2015. – Т. 98. – С. 391-398.

109. Tomio A. et al. Role of alloyed molybdenum on corrosion resistance of austenitic Ni–Cr–Mo–Fe alloys in H2S–Cl–environments //Corrosion Science. – 2015. – Т. 98. – С. 391-398.

110. Gao X., Liu M. Corrosion behavior of high-strength C71500 copper-nickel alloy in simulated seawater with high concentration of sulfide //Materials. – 2022. – Т. 15. – №. 23. – С. 8513.

111. Sun S. et al. Intergranular-stress corrosion cracking mechanism of brass in H2S environment: A DFT study //Computational Materials Science. – 2019. – Т. 170. – С. 109193.

112. Li H. et al. Molecular simulation on permeation behavior of CH4/CO2/H2S mixture gas in PVDF at service conditions //Polymers. – 2022. – Т. 14. – №. 3. – С. 545.

113. Maraveas C. Durability issues and corrosion of structural materials and systems in farm environment //Applied Sciences. – 2020. – Т. 10. – №. 3. – С. 990.

114. Hussain M. et al. Review of prediction of stress corrosion cracking in gas pipelines using machine learning //Machines. – 2024. – Т. 12. – №. 1. – С. 42.

115. Xie M., Tian Z. A review on pipeline integrity management utilizing in-line inspection data //Engineering Failure Analysis. – 2018. – Т. 92. – С. 222-239.

116. Vakili M. et al. Analysis, Assessment, and Mitigation of Stress Corrosion Cracking in Austenitic Stainless Steels in the Oil and Gas Sector: A Review //Surfaces (2571-9637). – 2024. – Т. 7. – №. 3.

117. Saji V. S. Corrosion Inhibitors in the Oil and Gas Industry.